ている。したがって、それらの酸化ストレスに対するフィードバック機構として TSA の発現が増加している可能性が考えられる.
今回同定された MDS に高発現している蛋白の機能解析を進めることは、MDS の診断あるいは治療の標的となる蛋白の同定につながるものと考える。 今後はさらに MDS の骨髄細胞を検体として、CD34 陽性細胞レベルでのプロテオーム解析も行い、本症の病因、病態に関与する蛋白の同定を進める予定である。

## E. 結論

MDS 患者と正常人における好中球の蛋白発現パターンを比較検討した結果、MDS 好中球において特異的に高発現している蛋白を数種類同定した。それらの蛋白の解析を進めることにより、MDS の病因、病態の一部が明らかになると考える。

## F. 健康危険情報

なし

## G. 研究発表

論文発表

1. Kazama H, Teramura M, Yoshinaga K, Kato T, Motoji T, Mizoguchi H. "Proteomics approach to identifying proteins abnormally expressed in neutrophils in patients with myelodysplastic syndrome. 8th International symposium on myelodysplastic syndromes." 2005 発表予定

## H. 知的財産権の出願・登録状況

1. 特許取得
2. 実用新案登録
3. その他

いずれも予定なし

厚生労働科学研究費補助金（難治性疾患克服研究事業）
分担研究報告書

# CGH アレイを用いた MDS の原因遺伝子の探索

分担研究者　小川誠司　東京大学医学部附属病院　造血再生医療寄付講座　客員助教授

**研究要旨**
骨髄異形成症候群(MDS)は染色体の増幅・欠失といった数的異常の頻度が高く、共通に変異の認められる領域に疾患の責任遺伝子が存在することが予想されている。そこでアレイ解析技術を用いて、MDS に生ずるゲノムのコピー数の微小な変化を網羅的に探索し、変化の集中する領域から MDS に対する分子標的薬剤の開発のターゲットとなる遺伝子を同定することを目指している。平成 16 年度には、まずヒト全ゲノムにわたって平均 1Mb の解像度の Human 1M アレイの作成とこれを用いた MDS 検体のゲノム解析を行い多数の微小な欠失や増幅を同定した。またこれらのコピー数の異常を認める領域の多くが症例間で共通していることが明らかとなった。現在、これらの領域について、その責任遺伝子の候補を同定する作業を進めている。さらにより高解像度の Affymetrix GeneChip を用いて、ゲノムコピー数の新規解析法の確立とその性能の検討を行った。まず独自に解析アルゴリズムの開発を行い、極めて精度の高いコピー数解析が可能となった。これにより、従来は全く不可能であったアレル別のコピー数の解析も可能となった。今後本アレイを用いて、より高密度に MDS 検体におけるコピー数の異常の網羅的解析を行い分子標的候補を同定し、分子標的薬の開発と疾患モデルマウスの作製に利用する。

## A．研究目的

難治性疾患である骨髄異形成症候群(MDS)は染色体異常を多症例で認めることを特徴とし、これらの異常の病態への関与が示唆されている。特に染色体の増幅・欠失といった数的異常の頻度が高く、共通に変異の認められる領域に疾患の責任遺伝子が存在することが予想されている。そこで MDS に対する分子標的薬剤の開発のターゲットとなる遺伝子を同定することを目的として、アレイ解析技術を用いて、MDS に生ずるゲノムのコピー数の微小な変化を網羅的に探索した。

## B．研究方法

(1) Human 1M アレイの作成とこれを用いた造血器腫瘍ゲノムの解析
FISH 法によって特異的なヒト染色体座が確認されている約 3200 個の BAC クローンを配置したアレイを大量に作製し、MDS 62 例を対象に、ゲノムコピー数の網羅的解析を行った。さらに複数の症例にて共通にコピー数の異常を認める領域を同定し、その領域内に存在する遺伝子を見出した。
(2) Affymetrix GeneChip を用いたゲノムコピー数の新規解析法の確立
同アレイでは、高密度に配置された SNP 特異的オリゴヌクレオチドプローブにより、全ゲノムについて 116204 個の遺伝子座について SNP タイピングを行うことが可能なシステムである。本アレイでは、検出される SNP シグナルに高い定量性が認められることから、同アレイを用いて MDS を含む腫瘍ゲノムのコピー数を高精度に解析するアルゴリズムの確立を試みた。

(倫理面への配慮)
検討に用いた検体は、当該患者からインフォームドコンセントを得たのちに連結可能匿名化を施して検討に用いた。当院の倫理委員会の承認済みである。

## C．研究結果

(1) 従来の染色体分析により繰り返し報告されてきた染色体セグメント単位での大きな異常に加えて、多数の微小な欠失や増幅が同定され、また、これらの多くが症例間で共通してコピー数の異常が認められることが明らかとなった。現在、これらの多数の領域について、その責任遺伝子の候補を同定する作業を進めている。
(2) 独自に解析アルゴリズムの開発を行い、Affymetrix GeneChip 用コピー数解析プログラムを構築した。アレイにより検出されるコピー数のシグナルを多重回帰により解析し種々の補正を行うことにより、解析のシグナル/ノイズ比は顕著に改善を認め、極めて精度の高いコピー数解析が可能となった。さらに、同アレイでは、膨大な SNP の多型情報が同時に得られることから、単なるコピー数の変化ではなく、従来は全く不可能であったアレル別のコピー数の解析も可能となった。

## D．考察

Human 1M アレイを用いた網羅的ゲノムコピー数の解析により、多数の微小な欠失や増幅が同定された。これらの領域に存在する遺伝子変異が MDS の病態に関与することが示唆される。例えば、8p の～200kb の増幅領域は、MDS の 30%程度で増幅が認められる領域で、白血病細胞株の検討においても骨髄系白血病に特異的に増幅

が認められる領域であるが、この領域の近傍にマップされる MASL1 遺伝子は、これまでにリンパ腫の一例で染色体転座により遺伝子発現の上昇が報告されており、MDS の発症進展に関与する遺伝子の重要な候補と考えられた。
また新たに Affymetrix 社のアレイを用いた解析法を確立したことにより、非常に微細なゲノムコピー数の解析が可能となり、最小 3.8kb の欠失まで確認されている。このアレイを用いた解析により、アレル別のコピー数の解析も可能となった。その結果、MDS 症例の一部では、コピー数の変化をともなうことなく LOH を示す領域が多数同定されることを見いだしている。これらの変異領域には、癌抑制遺伝子あるいは癌遺伝子が存在することが示唆される。

**E．結論**
自作した Human 1M アレイを用いて MDS 症例に共通に欠失・増幅を認める領域を同定した。さらに超高解像度の Affymetrix 社のアレイを用いた網羅的解析法を確立した。今後、本システムによって初めて実現した非常に微細なゲノムコピー数の解析を行い、治療標的分子の同定を目指す。これにより分子標的薬の開発と疾患モデルマウスの作製が可能となる。

**F．健康危険情報**
なし

**G．研究発表**
論文発表
1. Hosoya N, Qiao Y, Hangaishi A, Wang L, Nannya Y, Sanada S, Kurokawa M, Chiba S, Hirai H, Ogawa S. Identification of a SRC-like tyrosine kinase gene, FRK, fused with ETV6 in a patient with acute myelogenous leukemia carrying a t(6;12)(q21;p13) translocation. Genes Chromosomes Cancer 42: 269-279, 2004
2. Ichikawa M, Asai T, Chiba S, Kurokawa M, Ogawa S. Runx1/AML-1 ranks as a master regulator of adult hematopoiesis. Cell Cycle 3: 722-724, 2004
3. Ichikawa M, Asai T, Saito T, Yamamoto G, Seo S, Yamazaki I, Yamagata T, Mitani K, Chiba S, Ogawa S, Kurokawa M, Hirai H. AML-1 is required for megakaryocytic maturation and lymphocytic differentiation, but not for maintenance of hematopoietic stem cells in adult hematopoiesis. Nat Med 10: 299-304, 2004
学会発表
真田 昌、南谷 泰仁、半下石 明、細谷 紀子、王 莉莉、黒川 峰夫、千葉 滋、平井 久丸、小川 誠司。アレイCGHを用いた造血器腫瘍の網羅的ゲノム異常の解析。第63回日本癌学会学術総会 総会記事 p74, 2004

**H．知的財産権の出願・登録状況**
1. 特許取得
Affymetrix GeneChip 用コピー数解析プログラム CNAG (Copy Number Analyzer for Affymetrix® GeneChip® Mapping 100K arrays;特許出願予定 )
2. 実用新案登録
なし
3. その他
なし

# III. 研究成果の刊行に関する一覧

# 研究成果の刊行に関する一覧表（論文）

| 発表者氏名 | 論文タイトル名 | 発表誌名 | 巻名 | ページ | 出版年 |
|---|---|---|---|---|---|
| Ichikawa M, Asai T, Saito T, Yamamoto G, Seo S, Yamazaki I, Yamagata T, Mitani K, Chiba S, Ogawa S, Kurokawa M, Hirai H. (Author list corrected in Erratum, Nat Med 11:102, 2005) | AML-1 is required for megakaryocytic maturation and lymphocytic differentiation, but not for maintenance of hematopoietic stem cells in adult hematopoiesis. | Nat Med | 10 | 299-304 | 2004 |
| Maki K, Arai H, Waga K, Sasaki K, Nakamura F, Imai Y, Kurokawa M, Hirai H, Mitani K. | Leukemia-related transcription factor TEL is negatively regulated through ERK-induced phosphorylation. | Mol Cell Biol | 24 | 3227-3237 | 2004 |
| Mitani K. | Molecular mechanisms of leukemogenesis by AML1/EVI-1. | Oncogene | 23 | 4263-4269 | 2004 |
| Sasaki K, Nakamura Y, Maki K, Waga K, Nakamura F, Arai F, Imai Y, Hirai H, Mitani K. | Functional analysis of a dominant-negative ΔETS TEL/ETV6 isoform. | Biochem Biophys Res Comm | 317 | 1128-1137 | 2004 |
| Mitsuma A, Asano H, Kinoshita T, Murate T, Saito H, Stamatoyannopoulos G, Naoe T. | Transcriptional regulation of FKLF-2 (KLF13) gene in erythroid cells. | Biochimica Biophysica Acta | 1727 | 125-133 | 2005 |
| Asano H, Murate T, Naoe T, Saito H, Stamatoyannopoulos G. | Molecular cloning and characterization of ZFF29: a protein containing a unique Cys2 His2 zinc-finger motif. | Biochem J | 384 | 647-653 | 2004 |
| Abe A, Emi N, Kanie T, Imagama S, Kuno Y, Takahashi M, Saito H, Naoe T. | Expression cloning of oligomerization activated genes with cell-proliferating potency by pseudotype retrovirus vector. | Biochem Biophys Res Comm | 320 | 920-926 | 2004 |
| Kanie T, Abe A, Matsuda T, Kuno Y, Towatari M, Yamamoto T, Saito H, Emi N, Naoe T. | TEL-Syk fusion constitutively activates PI3-K/Akt, MAPK and JAK2-independent STAT5 signal pathways. | Leukemia | 18 | 548-555 | 2004 |
| Harada H, Harada Y, Niimi H, Kyo T, Kimura A, Inaba T. | High incidence of somatic mutations in the AML1/RUNX1 gene in myelodysplastic syndrome and low blast percentage myeloid leukemia with myelodysplasia. | Blood | 103 | 2316-2324 | 2004 |
| Matsunaga T, Inaba T, Matsui H, Okuya M, Kinoshita T, Miyajima A, Funabiki T, Endo M, Inukai T, Look AT, Kurosawa H. | Regulation of annexin II by cytokine-initiated signaling pathways and E2A-HLF oncoprotein. | Blood | 103 | 3185-3191 | 2004 |

# 研究成果の刊行に関する一覧表（論文）

| 発表者氏名 | 論文タイトル名 | 発表誌名 | 巻名 | ページ | 出版年 |
|---|---|---|---|---|---|
| Kuribara R, Honda H, Matsui H, Shinjyo T, Inukai T, Sugita K, Nakazawa S, Hirai H, Ozawa K, Inaba T. | Roles of Bim in apoptosis of normal and Bcr-Abl-expressing hematopoietic progenitors. | Mol Cell Biol | 24 | 6172-6183 | 2004 |
| Inukai T, Inaba T, Dang J, Kuribara R, Ozawa K, Miyajima A, Wu W, Look AT, Arinobu Y, Iwasaki H, Akashi K, Kagami K, Goi K, Sugita K, Nakazawa S. | TEF, an anti-apoptotic bZIP transcription factor related to the oncogenic E2A-HLF chimera, inhibits cell growth by down-regulating expression of the common β chain of cytokine receptors. | Blood | | (in press) | |
| Yokoyama T, Miyazawa K, Yoshida T, Ohyashiki K. | Combination of vitamin K2 plus imatinib mesylate enhances induction of apoptosis in small cell lung cancer cell lines. | Int J Oncol | 26 | 33-40 | 2005 |
| Yokoyama T, Miyazawa K, Kurakawa E, Nagate A, Shimamoto T, Iwaya K, Akata S, Aoshima M, Serizawa H, Ohyashiki K. | Interstitial pneumonia induced by imatinib mesylate: pathologic study demonstrates alveolar destruction and fibrosis with eosinophilic infiltration. | Leukemia | 18 | 645-646 | 2004 |
| Okabe S, Fukuda S, Kim YJ, Niki M, Pelus LM, Ohyashiki K, Pandolfi PP, Broxmeyer HE. | Stromal cell-derived factor-1alpha/ CL12-induced chemotaxis of T cells involves activation of the RasGAP- associated docking protein p62Dok-1. | Blood | 105 | 474-480 | 2004 |
| Sumi M, Tauchi T, Sashida G, Nakajima A, Gotoh A, Shin-Ya K, Ohyashiki JH, Ohyashiki K. | A G-quadruplex-interactive agent, telomestatin (SOT-095), induces telomere shortening with apoptosis and enhances chemosensitivity in acute myeloid leukemia. | Int J Oncol | 24 | 1481-1487 | 2004 |
| Ishii Y, Ito Y, Kuriyama Y, Tauchi T, Ohyashiki K. | Imatinib mesylate for chronic eosinophilic leukemia with myelofibrosis | Leukemia Res | 28 Suppl 1 | S79-S80 | 2004 |
| Hosoya N, Qiao Y, Hangaishi A, Wang L, Nannya Y, Sanada S, Kurokawa M, Chiba S, Hirai H, Ogawa S. | Identification of a SRC-like tyrosine kinase gene, FRK, fused with ETV6 in a patient with acute myelogenous leukemia carrying a t(6;12)(q21;p13) translocation. | Genes Chromosomes Cancer | 42 | 269-279 | 2004 |
| Ichikawa M, Asai T, Chiba S, Kurokawa M, Ogawa S. | Runx1/AML-1 ranks as a master regulator of adult hematopoiesis. | Cell Cycle | 3 | 722-724 | 2004 |

# Ⅳ．　研究成果の刊行物・別刷

# ERRATUM: AML-1 is required for megakaryocytic maturation and lymphocytic differentiation, but not maintenance of hematopoietic stem cells in adult hematopoiesis

M Ichikawa, T Asai, T Saito, G Yamamoto, S Seo, I Yamazaki, T Yamagata, K Mitani, S Chiba, H Hirai, S Ogawa & M Kurokawa
*Nat. Med.* **10**, 299–304 (2004)

In the original version of this article, the order in which the authors were listed was incorrect. The correct order is: Motoshi Ichikawa, Takahashi Asai, Toshiki Saito, Sachiko Seo, Ieharu Yamazaki, Tetsuya Yamagata, Kinuko Mitani, Shigeru Chiba, Seishi Ogawa, Mineo Kurokawa & Hisamaru Hirai.

# CORRIGENDUM: Historical Research Highlights: KSHV and cancer

*Nat. Med.* **10**, 1175 (2004)

In this highlight, Yuan Chang's name was spelled Yuan Chan.

nature medicine

# AML-1 is required for megakaryocytic maturation and lymphocytic differentiation, but not for maintenance of hematopoietic stem cells in adult hematopoiesis

Motoshi Ichikawa[1,7], Takashi Asai[1,7], Toshiki Saito[1], Go Yamamoto[1], Sachiko Seo[1], Ieharu Yamazaki[3], Tetsuya Yamagata[1,5], Kinuko Mitani[4], Shigeru Chiba[1], Hisamaru Hirai[1,6], Seishi Ogawa[1,2] & Mineo Kurokawa[1]



**Embryonic development of multilineage hematopoiesis requires the precisely regulated expression of lineage-specific transcription factors, including AML-1 (encoded by *Runx1*; also known as CBFA-2 or PEBP-2αB)[1–5]. *In vitro* studies and findings in human diseases, including leukemias[6,7], myelodysplastic syndromes[8] and familial platelet disorder with predisposition to acute myeloid leukemia (AML)[9], suggest that AML-1 has a pivotal role in adult hematopoiesis. However, this role has not been fully uncovered *in vivo* because of the embryonic lethality of *Runx1* knockout in mice. Here we assess the requirement of AML-1/*Runx1* in adult hematopoiesis using an inducible gene-targeting method[10]. In the absence of AML-1, hematopoietic progenitors were fully maintained with normal myeloid cell development. However, AML-1-deficient bone marrow showed inhibition of megakaryocytic maturation, increased hematopoietic progenitor cells and defective T- and B-lymphocyte development. AML-1 is thus required for maturation of megakaryocytes and differentiation of T and B cells, but not for maintenance of hematopoietic stem cells (HSCs) in adult hematopoiesis.**

Using the Cre-*lox*P sequence-specific recombination system, we generated mutant mice in which exon 5 of the *Runx1* gene could be selectively deleted by the expression of Cre recombinase (Fig. 1a). We mated mutant animals carrying deleted (*Runx1*$^{-}$) or *lox*P-flanked (*Runx1*$^{fl}$) alleles, and observed lethal bleeding of *Runx1*$^{-/-}$ embryos as anticipated[1,2]. In contrast, *Runx1*$^{fl/fl}$ and *Runx1*$^{fl/-}$ mice were normal (data not shown). We then bred the mutant mice with *Mx-cre*-transgenic mice to generate *Runx1*$^{fl/+}$*Mx-cre* or *Runx1*$^{fl/-}$*Mx-cre* mice. In these mice, the *Runx1*$^{fl}$ allele could be effectively deleted in hematopoietic progenitors by using injected polyinosinic-polycytidylic acid (pIpC) to induce expression of Cre recombinase[10]. Two months after pIpC injection, genomic Southern blot analysis of *Runx1*$^{fl/-}$*Mx-cre* mice revealed that ≥90% of the bone marrow or peritoneal exudative cells, ~80% of which were morphologically normal neutrophils, had biallelic *Runx1* deletion. This indicates that *Runx1* deletion was induced in most bone marrow cells, and that most myeloid progenitors lacking AML-1 could still differentiate into mature neutrophils (Fig. 1b,c). Efficient excision of one *Runx1* allele was observed in the hematopoietic cells, including lymphocytes, of *Runx1*$^{fl/+}$*Mx-cre* mice. In contrast, only 9%, 32% and 57% of the thymocytes, splenic T cells and B cells *of Runx1*$^{fl/-}$*Mx-cre* mice, respectively, had a *Runx1*$^{-/-}$ genotype. Therefore, a large proportion of mature lymphocytes originated from lymphoid progenitor cells still expressing intact AML-1, and AML-1 deficiency should be disadvantageous to lymphocyte development.

Injection of pIpC did not cause significant differences in neutrophil counts or hemoglobin levels among the *Runx1*$^{fl/-}$*Mx-cre* (floxed) mice, *Runx1*$^{fl/+}$*Mx-cre* mice and *Runx1*$^{+/+}$*Mx-cre* (control) mice (Fig. 2a). Immediately after pIpC injection, however, platelet counts for the floxed mice declined to one-third to one-sixth of those for the control mice (Fig. 2a). Lymphocyte counts were slightly depressed after more than 4 weeks in the floxed and *Runx1*$^{fl/+}$*Mx-cre* mice. These results suggest that AML-1 is required for the maintenance of platelets and lymphocytes, but not for the sustained production of erythrocytes and neutrophils.

We next examined bone marrow cell morphology in the pIpC-treated floxed mice to determine whether thrombocytopenia results from abnormal megakaryopoiesis. The cellularity of the bone marrow and morphology of myeloid cells in the floxed mice were not remarkably altered from those of the control mice, except for a slightly elevated myeloid-erythroid ratio (2.35 ± 0.70 in floxed mice compared with 1.71 ± 0.39 in control mice; $n = 7$ (paired), $P = 0.046$ by Wilcoxon signed-rank test; Fig. 2b and data not shown). However, Wright-Giemsa staining of floxed bone marrow revealed the absence of normal megakaryocytes with abundant cytoplasm and lobulated nuclei (Fig. 2b). Instead, the floxed bone marrow contained a small number of immature megakaryocyte-like cells with occasionally sep-

[1]Department of Hematology and Oncology and [2]Department of Regeneration Medicine for Hematopoiesis, Graduate School of Medicine, University of Tokyo, 7-3-1 Hongo, Bunkyo-ku, Tokyo, 113-8655, Japan. [3]Department of Clinical Laboratory and Pathology, Inoue Memorial Hospital, 1-16 Shindencho, Chuo-ku, Chiba, 260-0027, Japan. [4]Department of Hematology, Dokkyo University School of Medicine, 800 Kitakobayashi, Mibu, Tochigi, 321-0293, Japan. [5]Present address: Immunology section, Joslin Diabetes Center, Harvard Medical School, One Joslin Place, Boston, Massachusetts 02215, USA. [6]Deceased. [7]These authors contributed equally to this work. Correspondence should be addressed to S.O. (sogawa-tky@umin.ac.jp).

Published online 15 February 2004; doi:10.1038/nm997

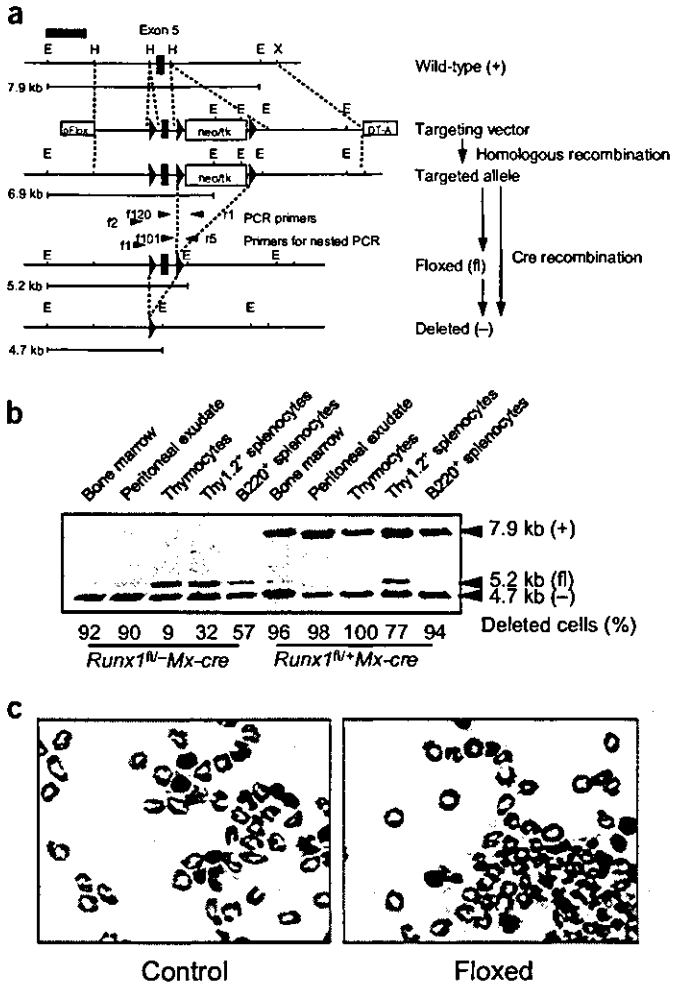


**Figure 1** Inducible AML-1 knockout mice. (**a**) Schematic representation of conditional gene targeting of the *Runx1* gene. E, *Eco*RI; H, *Hind*III; X, *Xba*I; gray box in upper left corner, 5′ genomic probe; *neo/tk*, PGK-*neo*/HSV-thymidine kinase positive selection cassette; *DT-A*, diphtheria toxin A chain negative selection cassette. (**b**) Southern blot genotyping of cells from hematopoietic organs of mice injected with pIpC. Numbers below lanes indicate proportion of *Runx1*-deleted cells. (**c**) Wright-Giemsa-stained, cytocentrifuged specimens of peritoneal inflammatory cells genotyped in **b**.

arated round nuclei, resembling the abnormal 'micromegakaryocytes' observed in human myelodysplastic syndromes (Fig. 2b). Consistent with this observation, a substantial increase in the number of small megakaryocytes was revealed in the floxed bone marrow by acetylcholinesterase staining, which specifically detects mature and immature megakaryocytes[11] (Fig. 2b).

Given the prominent immaturity of megakaryocytes in the floxed mice, we examined the ultrastructure of the megakaryocytes (Fig. 2c). In addition to their smaller size, floxed megakaryocytes showed poorly developed demarcation membranes compared with megakaryocytes from control (*Runx1*$^{+/+}$*Mx*$^{+}$*cre*) mice. During the maturation process, megakaryocytes acquire high DNA ploidy (>4*n*) through a cell cycle process known as endomitosis[12]. As expected from the smaller size of their nuclei, CD41$^{+}$ megakaryocytes from the floxed mice showed a markedly lower level of polyploidy (≤8*n*) than megakaryocytes from the control mice (modal ploidy, 16*n*), as revealed by flow cytometric measurement of DNA content. This demonstrates that AML-1 deletion also causes defective polyploidization in megakaryocytes (Fig. 2d). Although a recent report showed that AML-1 regulates the expression of megakaryocyte-specific genes in cooperation with GATA-1 (ref. 13), and although the small and immature megakaryocytes that we observed are reminiscent of those found in GATA-1 knockdown mice[14,15], the expression levels of megakaryocyte-specific transcription factors in floxed mice, including GATA-1, FOG-1 and NF-E2, remained unaffected according to RT-PCR analyses of lineage-negative (Lin$^{-}$) bone marrow cells (data not shown).

We subsequently conducted *in vitro* colony-forming assays to evaluate the frequency of hematopoietic progenitors. Floxed bone marrow cells formed more megakaryocytic colonies (CFU-Meg) than control bone marrow cells in semisolid media (Fig. 3a). The numbers of myeloid and mixed (myeloid and erythroid) colonies were also elevated in the floxed bone marrow. Using single-colony PCR genotyping, we detected the *Runx1*$^{-/-}$ genotype in 149 of 150 myeloid colonies, 48 of 50 erythroid colonies, 35 of 36 mixed colonies and 14 of 14 megakaryocytic colonies from pIpC-treated floxed bone marrow cells, thus excluding the possibility that those hematopoietic cells might be predominantly derived from progenitor cells still expressing intact AML-1 (data not shown). Using flow cytometry (Fig. 3b), we observed an increased number of cells in the Lin–c-Kit$^{hi}$CD41$^{hi}$ fraction, which was presumed to contain CFU-Meg[16], in the floxed bone marrow. Similarly, the number of cells defined by CD34-Lin$^{-/lo}$c-Kit$^{hi}$Sca-1$^{hi}$ (Fig. 3c), which represent the most immature hematopoietic progenitor cell population[17], was also elevated in the floxed bone marrow. Although development of both T and B cells from AML-1-deficient cells was impaired (Fig. 1b), the cells defined by Lin$^{-/lo}$IL-7Rα$^{+}$Sca-1$^{lo}$c-Kit$^{lo}$, previously reported to include common lymphocyte progenitors (CLPs)[18], were maintained in the floxed bone marrow (Fig. 3d).

Increased numbers of primitive hematopoietic progenitors, immortalized myeloid progenitor cells and arrested myeloid maturation have been observed in mice expressing the leukemic AML-1/ETO chimeric protein[19–21], which dominantly suppresses the normal function of AML-1. We observed an elevated colony-replating capacity of *Runx1*$^{-/-}$ hematopoietic cells, although replating could be repeated for only 2 months (Fig. 3e). Although AML-1-null neutrophils were morphologically normal, and freshly collected floxed bone marrow cells did not show altered apoptosis when assessed by annexin-V expression (data not shown), we detected increased apoptosis of myeloid colony-forming cells, suggesting that a certain degree of maturation arrest occurs in the myeloid lineage in the absence of AML-1 (Fig. 3f).

Because immature hematopoietic progenitor cell fractions were elevated in the floxed bone marrow, we used a competitive repopulation assay to assess their ability to reconstitute adult hematopoiesis[22]. We used isotypes of the pan-hematopoietic marker CD45 (Ly5) to distinguish the origins of the repopulating cells. Sublethally irradiated C57BL/6-Ly5.1 recipient mice (Ly5.1$^{+}$Ly5.2$^{-}$) were intravenously injected with a mixture of bone marrow cells from C57BL/6-Ly5.1/Ly5.2 $F_1$ competitor mice (Ly5.1$^{+}$Ly5.2$^{+}$) or floxed or control mice (Ly5.1$^{-}$Ly5.2$^{+}$) previously injected with pIpC. We then analyzed Ly5 isotypes on the repopulating cells by flow cytometry (Fig. 4a). Notably, the floxed bone marrow cells reconstituted neither peripheral T (Thy-1.2$^{+}$) nor B (B220$^{+}$) cells, whereas there were no significant differences in the mature neutrophil (Gr-1$^{hi}$Mac-1$^{+}$) and monocyte populations (Gr-1$^{lo}$Mac-1$^{+}$)[23] (Fig. 4a). The contribution to the reconstituted bone marrow was not significantly different in neutrophils (test/competitor = 0.382 ± 0.083 for floxed mice ($n$ = 8),

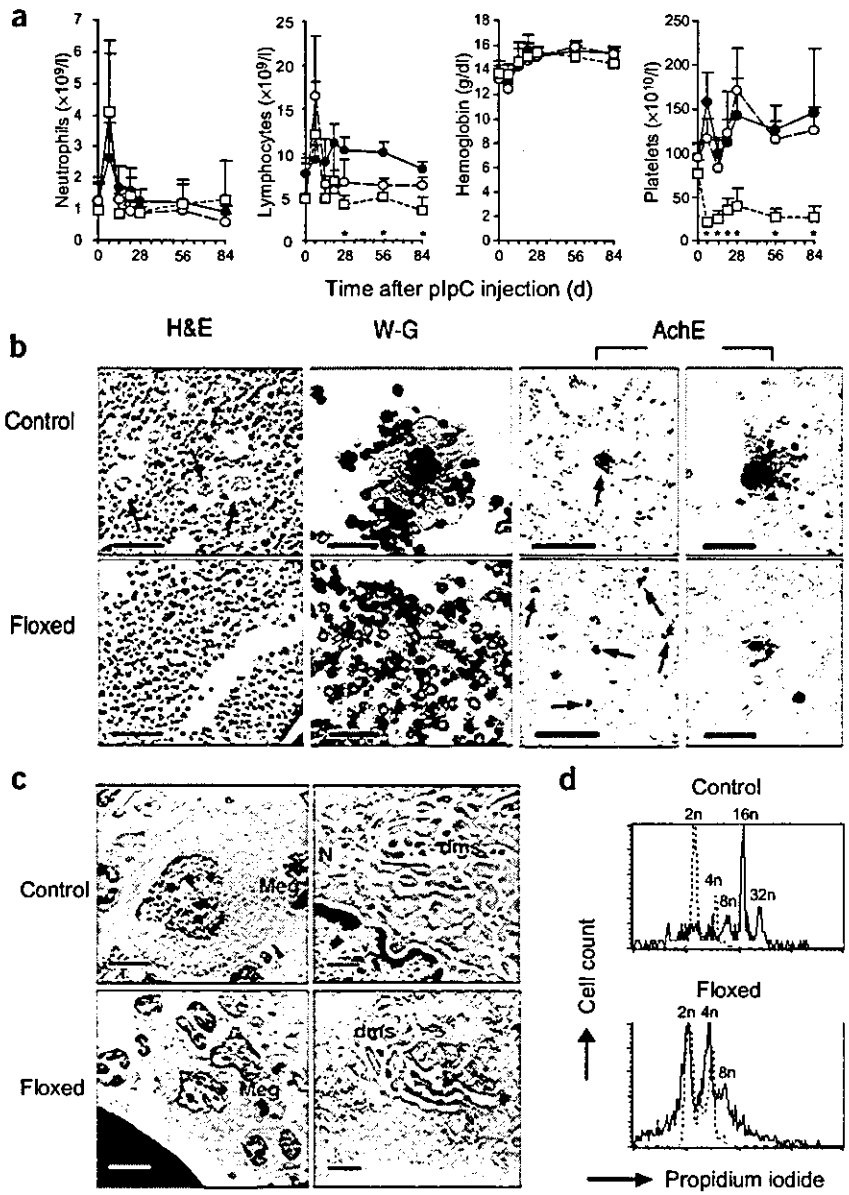


**Figure 2** Thrombocytopenia and megakaryocytic maturation arrest of induced AML-1 knockout mice. (a) Peripheral blood cell counts of *Runx1*$^{+/+}$*Mx-cre* (control; ●), *Runx1*$^{fl/+}$*Mx-cre* (○) and *Runx1*$^{fl/-}$*Mx-cre* (floxed; □) mice injected with pIpC on days 0, 2 and 4. Results are shown as mean + s.d. (error bars) from four to seven mice. *, $P < 0.01$ for floxed compared with control mice (unequal-variance *t*-test). (b) Histochemical analyses of bone marrow. W-G, Wright-Giemsa; AchE, acetylcholinesterase. Arrows indicate megakaryocytes. Scale bars, 50 μm (H&E, W-G, and AchE right panel) or 250 μm (AchE left panel). (c) Electron micrographs of bone marrow megakaryocytes. Meg/arrowhead, megakaryocytes; dms, demarcation membranes; N, nucleus. Scale bars, 5 μm (left) or 500 nm (right). (d) DNA contents of CD41$^+$ bone marrow cells. – – –, CD41$^-$ fractions for 2*n* and 4*n* controls. Typical results from three experiments are shown (4–8 weeks after pIpC injection).

compared with 0.424 ± 0.118 for control mice ($n = 4$); $P = 0.93$ by Wilcoxon rank-sum test) or monocytes (test/competitor = 0.443 ± 0.082 for floxed mice ($n = 8$), compared with 0.940 ± 0.440 for control mice ($n = 4$); $P = 0.35$). The floxed cells also repopulated the megakaryocytic progenitors (Lin$^-$CD41$^+$; Fig. 4b). Given the inability of AML-1-deficient cells to reconstitute the T-cell lineage, we investigated thymocyte development in the absence of AML-1 by analyzing double-negative thymocytes of the recipient mice. We observed a significant block in the maturation of floxed T-cell progenitors at the transition from CD44$^+$CD25$^+$ (DN2) to CD44$^-$CD25$^+$ (DN3) (DN3/DN2 ratio of Ly5.1$^-$Ly5.2$^+$ cells = 0.025 ± 0.029 for floxed mice ($n = 5$), compared with 1.87 ± 1.51 for control mice ($n = 4$); $P < 0.05$; Fig. 4c), indicating that immature T-cell precursors had accumulated in the thymus. These findings, along with the observation that the CLP fraction was not affected in the floxed bone marrow, suggest that AML-1 is not necessary for the maintenance of CLPs, but is required in lymphoid precursors committed to T- or B-cell lineages. Consistent with this, a recent report and our experiments using *lck-Cre*-mediated, T-cell-specific AML-1-knockout mice show that the maturation of T-cell progenitors deficient in AML-1 is blocked at the DN3-DN4 transition (ref. 24 and T.A. *et al.*, unpublished data). Because *lck-Cre* expression becomes evident at the DN3 stage or later, the present study unveiled an important role of AML-1 in the DN2-DN3 transition. However, because of the insufficient contribution of the floxed cells to the B220$^+$ bone marrow fraction (test/competitor = 0.011 ± 0.012 ($n = 8$) compared with 0.306 ± 0.295 for control ($n = 4$)), we could not determine which step in B-cell development was affected by the absence of AML-1. The role of AML-1 in B-cell development might be revealed by other approaches, including the analysis of B-cell lineage-specific AML-1-knockout mice. Although lymphocyte development is substantially blocked at early stages in the absence of AML-1, the detection of AML-1-deleted T and B cells in the periphery of *Runx1*$^{fl/-}$*Mx-cre* mice (Fig. 1b) indicates that some lymphoid progenitors may still survive for a prolonged period and differentiate into mature lymphocytes.

Our data show that lack of AML-1 at the adult stage causes hematopoietic progenitor cell expansion, probably through a partial block in myeloid cell differentiation. This finding agrees with the phenotypes of previously reported mouse models of t(8;21)—carrying human leukemia, in which AML-1/ETO fusion protein is implicated in leukemogenesis through dominant-negative suppression of AML-1 function[19–21]. The loss or dominant-negative suppression of AML-1 function is also found in human myelodysplastic syndromes and familial platelet disorder with predisposition to AML[8,9], both of which are thought to be a preleukemic state. Taken as a whole, our observations suggest that the number of hematopoietic progenitor cells is negatively regulated by AML-1, and that the loss of AML-1 function triggers a preleukemic state. However, the myeloid immaturity and immortalization of bone marrow progenitors observed in AML-1/ETO mice could not be recapitulated in our *Runx1*$^{fl/-}$*Mx-cre* mice. Therefore, AML-1/ETO may not only inhibit AML-1 function, but

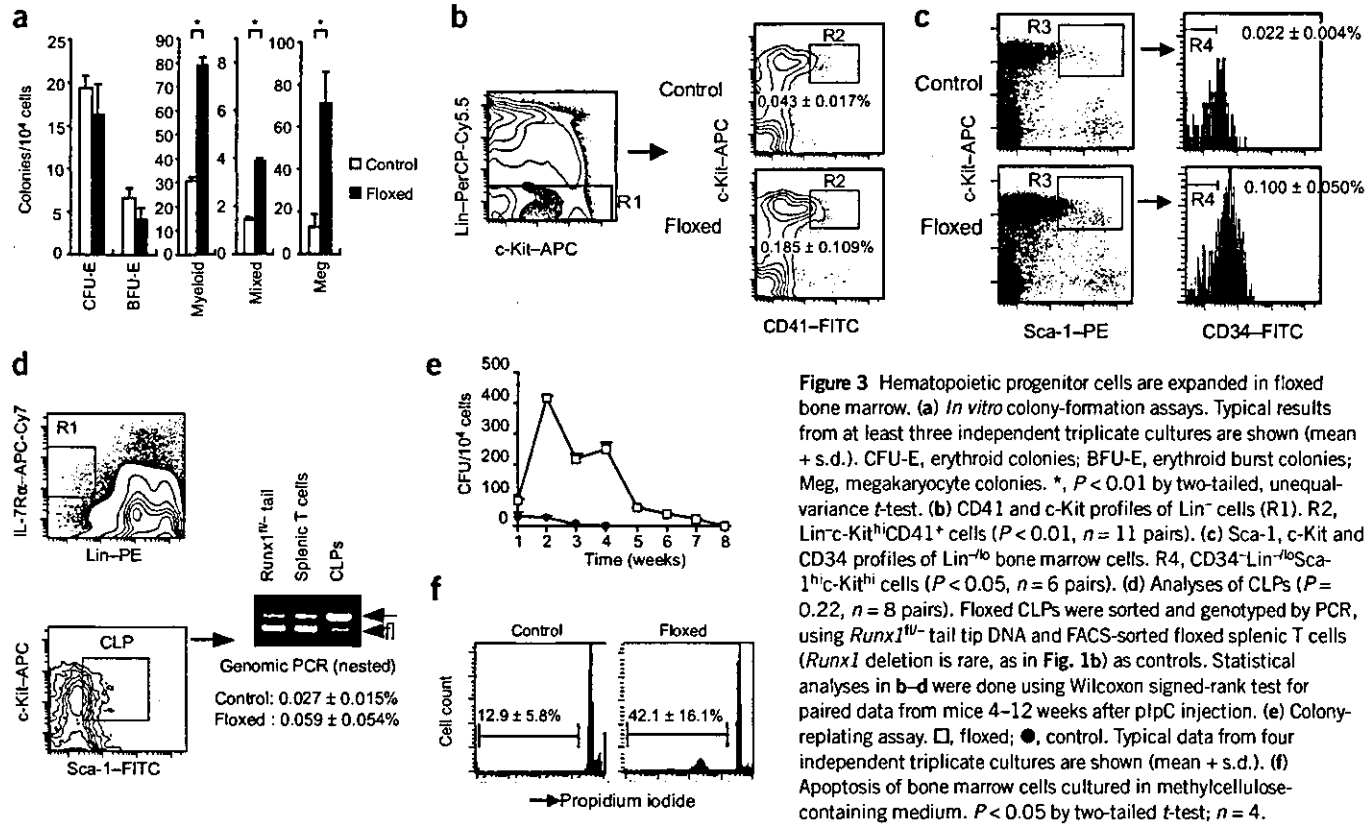


**Figure 3** Hematopoietic progenitor cells are expanded in floxed bone marrow. **(a)** *In vitro* colony-formation assays. Typical results from at least three independent triplicate cultures are shown (mean + s.d.). CFU-E, erythroid colonies; BFU-E, erythroid burst colonies; Meg, megakaryocyte colonies. *, $P < 0.01$ by two-tailed, unequal-variance *t*-test. **(b)** CD41 and c-Kit profiles of Lin⁻ cells (R1). R2, Lin⁻c-Kit$^{hi}$CD41$^{+}$ cells ($P < 0.01$, $n = 11$ pairs). **(c)** Sca-1, c-Kit and CD34 profiles of Lin$^{-/lo}$ bone marrow cells. R4, CD34⁻Lin$^{-/lo}$Sca-1$^{hi}$c-Kit$^{hi}$ cells ($P < 0.05$, $n = 6$ pairs). **(d)** Analyses of CLPs ($P = 0.22$, $n = 8$ pairs). Floxed CLPs were sorted and genotyped by PCR, using *Runx1*$^{fl/-}$ tail tip DNA and FACS-sorted floxed splenic T cells (*Runx1* deletion is rare, as in **Fig. 1b**) as controls. Statistical analyses in **b–d** were done using Wilcoxon signed-rank test for paired data from mice 4–12 weeks after pIpC injection. **(e)** Colony-replating assay. □, floxed; ●, control. Typical data from four independent triplicate cultures are shown (mean + s.d.). **(f)** Apoptosis of bone marrow cells cultured in methylcellulose-containing medium. $P < 0.05$ by two-tailed *t*-test; $n = 4$.

may also have the ability to immortalize hematopoietic progenitors.

Although AML-1 is considered to be a master regulator of definitive hematopoiesis, our current study shows that AML-1 is dispensable for prolonged hematopoietic cell engraftment, as well as commitment to the myeloid lineage and at least to double-negative thymocytes in the lymphoid lineage. Our present data also indicate that AML-1 is essential for the terminal differentiation of hematopoietic progenitors of megakaryocytic and lymphocytic lineages, which establishes AML-1 as a regulator with multiple roles in the maintenance of lineage-committed cells in adult hematopoiesis. However, our results also suggest that the maintenance of HSCs and their commitment to more mature progenitors in adult hematopoiesis does not always require a transcription factor essential for hematopoietic ontogeny during embryogenesis, and can be induced by other hematopoietic genes. This is supported by a previous study that showed that SCL/*tal-1*, a transcription factor essential for the devel-

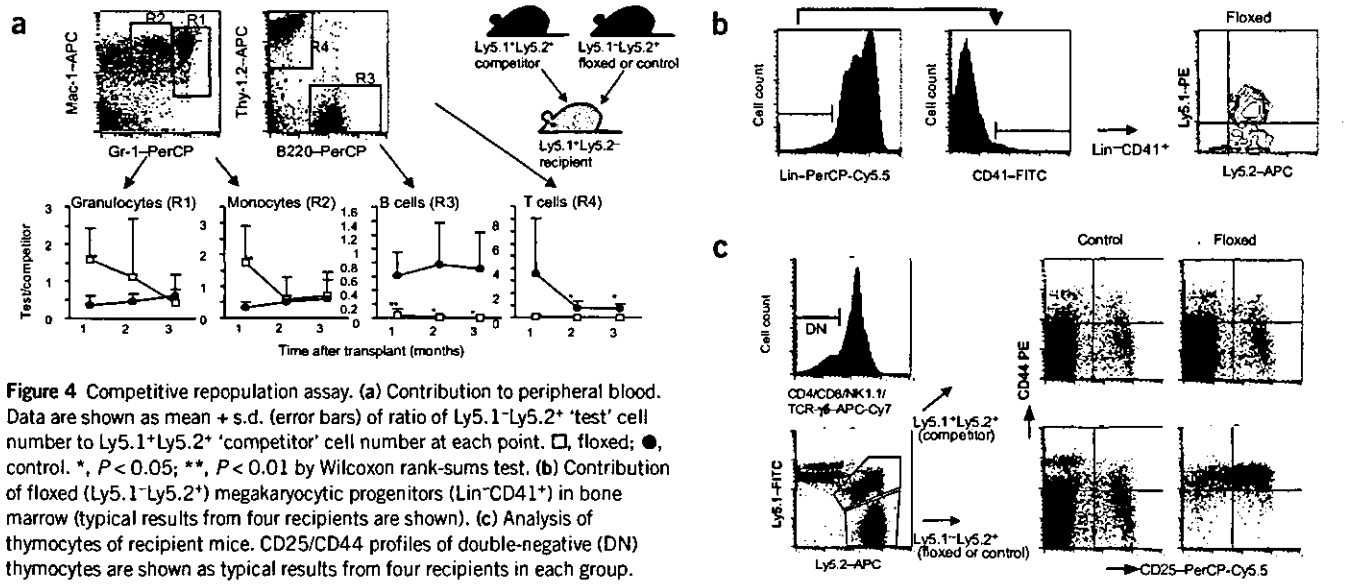


**Figure 4** Competitive repopulation assay. **(a)** Contribution to peripheral blood. Data are shown as mean + s.d. (error bars) of ratio of Ly5.1⁻Ly5.2⁺ 'test' cell number to Ly5.1⁺Ly5.2⁺ 'competitor' cell number at each point. □, floxed; ●, control. *, $P < 0.05$; **, $P < 0.01$ by Wilcoxon rank-sums test. **(b)** Contribution of floxed (Ly5.1⁻Ly5.2⁺) megakaryocytic progenitors (Lin⁻CD41⁺) in bone marrow (typical results from four recipients are shown). **(c)** Analysis of thymocytes of recipient mice. CD25/CD44 profiles of double-negative (DN) thymocytes are shown as typical results from four recipients in each group.

opment of primitive hematopoiesis during the embryonic stage, is required for the proper differentiation of erythroid and megakaryocytic lineages, but not for the maintenance of HSCs in adult hematopoiesis[25]. To fully understand the intricate process of hematopoiesis, it will be necessary to determine the roles of those hematopoietic genes.

## METHODS

**Mice.** We introduced the targeting vector (Fig. 1a) into TT2 embryonic stem cells[26], and transiently expressed Cre recombinase to generate embryonic stem cell lines carrying the *Runx1*$^{fl}$ or *Runx1*$^{-}$ alleles. Chimeric mice raised by aggregation were crossed to the C57BL/6 background, and were mated to interferon-inducible *Mx-cre* transgenic mice[10]. *Mx-cre* expression was induced by intraperitoneally injecting 250 μg of pIpC, on three alternate days, into 4- to 8-week-old mice[10]. C57BL/6-Ly5.1 congenic and C57BL/6-Ly5.1/Ly5.2 $F_1$ mice were used for competitive repopulation assays. Mice were kept at the Animal Center for Biomedical Research, University of Tokyo, according to institutional guidelines.

**Genotyping.** For PCR genotyping, cells were lysed in a lysis buffer (0.3% Tween 20, 0.3% NP-40, and 120 μg/ml proteinase K in 1× TE buffer) at 55 °C for 1 h, followed by inactivation at 80 °C for 10 min. DNA was amplified using primers f2 (5′-ACAAAACCTAGGTGTACCAGGAGAACAAGT-3′), f120 (5′-CCCTGAAGACAGGAGAAGTTTCCA-3′) and r1 (5′-GTCTACTCCTTGCCTCAGAAAACAAAAAC-3′) for the first PCR reaction, and nested primers f1 (5′-AAAACCTAGGTGTACCAGGAGAACAAGTC-3′), f101 (5′-TTCCAGGTCAACTCTCTCACCTCTC-3′) and r5 (5′-ATCTGAGTTGGCCTAATTTCCCTTTG-3′) for the second reaction, to detect the 280-base pair *Runx1*$^{-}$ and 220-base pair *Runx1*$^{fl}$ products. Southern blot analyses of DNA samples digested with *Eco*RI were done according to standard protocols, using a 5′ *Eco*RI-*Bgl*II genomic probe (Fig. 1a).

**Analyses of blood cells.** Peripheral blood was counted using an automated hemacytometer, and leukocytes were morphologically classified to calculate neutrophil and lymphocyte counts. Mice were analyzed for bone marrow morphology 2 months after pIpC administration. For histological examination, sectioned femoral bone marrow specimens were stained with H&E, and cytocentrifuged specimens were stained with Wright-Giemsa or for acetylcholinesterase as previously described[11]. Peritoneal exudative cells were collected by washing the peritoneal cavities of mice 4 h after intraperitoneal injection of 2 ml of 2% casein in PBS. Splenocytes were labeled with antibodies to Thy-1.2 (for T cells) or B220 (for B cells), conjugated to magnetic microbeads to collect splenic lymphocytes using a MACS LS+ system (Miltenyi Biotec). The cells were checked for purity by flow cytometry (>97%; data not shown).

**Ultrastructural studies.** Femoral bone marrow samples prepared 4 weeks after pIpC injection as previously described[27] were examined with a JEOL 1200CX electron microscope.

**Flow cytometry and cell sorting.** All monoclonal antibodies and fluorochromes were purchased from BD PharMingen. To measure bone marrow progenitor cells other than CLPs, cells were stained with FITC-conjugated antibodies to CD41 or CD34, phycoerythrin (PE)-conjugated antibody to Sca-1, allophycocyanin (APC)-conjugated antibody to c-Kit, and biotin-conjugated antibodies to lineage (Lin) markers (CD3ε, CD4, CD8a, B220, Gr-1, Mac-1 and Ter119), and visualized with streptavidin-PerCP-Cy5.5. For CLP cell fractions, cells were stained with Lin-PE, Sca-1-FITC, c-Kit-APC and IL-7Rα–biotin/streptavidin-APC-Cy7. Stained samples were analyzed using either FACSCalibur or BD LSRII (BD Biosciences). For sorting CLP cells, Lin$^{+}$ were predepleted from bone marrow cells using the MACS LD system (Miltenyi Biotec). The remaining fraction was stained for CLP as described above and sorted using a FACSVantage cell sorter. The cell sorter was calibrated to achieve >98% purity for Thy-1.2$^{+}$ cells stained with Thy-1.2–APC. Approximately 1,000 CLP cells were genotyped by PCR. To analyze competitively repopulated cells, cells were stained with Ly5.2–FITC, Ly5.1–PE, Gr-1–biotin/streptavidin–PerCP and Mac-1–APC for myeloid cells, and with Ly5.2–FITC, Ly-5.1–PE, B220–PerCP and Thy-1.2–APC for T and B lymphocytes. Thymocytes were stained with Ly5.1–FITC, Ly5.2–APC, CD25– PerCP-Cy5.5, CD44–PE and biotin-conjugated antibodies to CD4, CD8, NK1.1 and TCR-γδ, and visualized by streptavidin–APC-Cy7 for analyzing double-negative thymocytes. Bone marrow megakaryocytic progenitors were stained with CD41–FITC, Ly-5.1–PE, Ly-5.2–APC and Lin–biotin/streptavidin-PerCP-Cy5.5. Two-color flow cytometric analysis of the DNA content of bone marrow megakaryocytes stained with CD41–FITC was performed as previously described[28].

***In vitro* hematopoietic colony-forming assays.** For CFU-Meg, $2.5 \times 10^4$ bone marrow cells from mice 4–8 weeks after pIpC injection were cultured in 1 ml of α-MEM containing 0.8% methylcellulose, 1% BSA, 30% FBS, 100 μM 2-mercaptoethanol and 10 units of mouse thrombopoietin. For other (myeloid and erythroid) colonies, $5 \times 10^4$ cells were cultured in 1 ml of IMDM containing 0.8% methylcellulose, 1% BSA, 30% FBS, 100 μM 2-mercaptoethanol, 100 ng/ml of mouse stem cell factor, 5 ng/ml of mouse interleukin-3 and 7.5 units/ml of human erythropoietin (all growth factors were generously provided by Kirin Brewery). Colonies were counted after 3 d (for erythroid colonies), 5 d (for erythroid bursts and myeloid colonies), 7 d (for mixed colonies) or 8 d (for CFU-Meg) of culture in 5% $CO_2$ at 37 °C. For replating experiments, the whole myeloid and erythroid culture was pooled on day 7 and washed twice, and $1 \times 10^4$ cells were subjected to subsequent culture in the same medium. Scoring for colonies and reculturing were repeated every 7 d.

**Detection of apoptotic cells.** Whole myeloid and erythroid methylcellulose cultures were pooled on day 7 of culture, washed, fixed and stained with propidium iodide for analysis by flow cytometry to detect apoptotic cells (DNA content < 2*n*) as previously described[29].

**Competitive repopulation assay.** X-ray-irradiated (9.5 Gy, 0.3 Gy/min, unfractionated) recipient mice were intravenously injected with a mixture of $1 \times 10^5$ each of unfractionated bone marrow cells from 'test' mice (floxed or control mice, 8–12 weeks after pIpC injection) and competitor mice. Peripheral blood was analyzed monthly, and bone marrow cells and thymocytes were analyzed 3 months after transplantation by flow cytometry.

ACKNOWLEDGMENTS

We thank S. Aizawa for providing us with TT2 ES cells; T. Komori for *Runx1* genomic fragments; J. Takeda for *Mx-cre*-transgenic mice; and thank K. Kumano, A. Kunisato and other members of H.H.'s lab for critical discussion. This work was supported in part by a Grant-in-Aid for Scientific Research (KAKENHI 13307029, 15689015) from the Japan Society for the Promotion of Science, and by Health and Labour Sciences Research grants from the Ministry of Health, Labour and Welfare.

COMPETING INTERESTS STATEMENT

The authors declare that they have no competing financial interests.

Received 4 November 2003; accepted 20 January 2004
Published online at http://www.nature.com/naturemedicine/

1. Okuda, T., van Deursen, J., Hiebert, S.W., Grosveld, G. & Downing, J.R. AML1, the target of multiple chromosomal translocations in human leukemia, is essential for normal fetal liver hematopoiesis. *Cell* **84**, 321–330 (1996).
2. Wang, Q. *et al.* Disruption of the *Cbfa2* gene causes necrosis and hemorrhaging in the central nervous system and blocks definitive hematopoiesis. *Proc. Natl. Acad. Sci. USA* **93**, 3444–3449 (1996).
3. Mukouyama, Y. *et al.* The AML1 transcription factor functions to develop and maintain hematogenic precursor cells in the embryonic aorta-gonad-mesonephros region. *Dev. Biol.* **220**, 27–36 (2000).
4. Yokomizo, T. *et al.* Requirement of Runx1/AML1/PEBP2αB for the generation of haematopoietic cells from endothelial cells. *Genes Cells* **6**, 13–23 (2001).
5. North, T.E. *et al.* Runx1 expression marks long-term repopulating hematopoietic stem cells in the midgestation mouse embryo. *Immunity* **16**, 661–672 (2002).
6. Tenen, D.G., Hromas, R., Licht, J.D. & Zhang, D.E. Transcription factors, normal myeloid development, and leukemia. *Blood* **90**, 489–519 (1997).
7. Lutterbach, B. & Hiebert, S.W. Role of the transcription factor AML-1 in acute leukemia and hematopoietic differentiation. *Gene* **245**, 223–235 (2000).
8. Imai, Y. *et al.* Mutations of the AML1 gene in myelodysplastic syndrome and their functional implications in leukemogenesis. *Blood* **96**, 3154–3160 (2000).
9. Song, W.J. *et al.* Haploinsufficiency of CBFA2 causes familial thrombocytopenia with propensity to develop acute myelogenous leukaemia. *Nat. Genet.* **23**, 166–175 (1999).

10. Kuhn, R., Schwenk, F., Aguet, M. & Rajewsky, K. Inducible gene targeting in mice. *Science* **269**, 1427–1429 (1995).
11. Jackson, C.W. Cholinesterase as a possible marker for early cells of the megakaryocytic series. *Blood* **42**, 413–421 (1973).
12. Kaushansky, K. The enigmatic megakaryocyte gradually reveals its secrets. *Bioessays* **21**, 353–360 (1999).
13. Elagib, K.E. *et al.* RUNX1 and GATA-1 coexpression and cooperation in megakaryocytic differentiation. *Blood* **101**, 4333–4341 (2003).
14. Shivdasani, R.A., Fujiwara, Y., McDevitt, M.A. & Orkin, S.H. A lineage-selective knockout establishes the critical role of transcription factor GATA-1 in megakaryocyte growth and platelet development. *EMBO J.* **16**, 3965–3973 (1997).
15. Takahashi, S. *et al.* Role of GATA-1 in proliferation and differentiation of definitive erythroid and megakaryocytic cells *in vivo*. *Blood* **92**, 434–442 (1998).
16. Hodohara, K., Fujii, N., Yamamoto, N. & Kaushansky, K. Stromal cell-derived factor-1 (SDF-1) acts together with thrombopoietin to enhance the development of megakaryocytic progenitor cells (CFU-MK). *Blood* **95**, 769–775 (2000).
17. Osawa, M., Hanada, K., Hamada, H. & Nakauchi, H. Long-term lymphohematopoietic reconstitution by a single CD34-low/negative hematopoietic stem cell. *Science* **273**, 242–245 (1996).
18. Kondo, M., Weissman, I.L. & Akashi, K. Identification of clonogenic common lymphoid progenitors in mouse bone marrow. *Cell* **91**, 661–672 (1997).
19. Rhoades, K.L. *et al.* Analysis of the role of AML1-ETO in leukemogenesis, using an inducible transgenic mouse model. *Blood* **96**, 2108–2115 (2000).
20. Higuchi, M. *et al.* Expression of a conditional AML1-ETO oncogene bypasses embryonic lethality and establishes a murine model of human t(8;21) acute myeloid leukemia. *Cancer Cell* **1**, 63–74 (2002).
21. de Guzman, C.G. *et al.* Hematopoietic stem cell expansion and distinct myeloid developmental abnormalities in a murine model of the AML1-ETO translocation. *Mol. Cell. Biol.* **22**, 5506–5517 (2002).
22. Szilvassy, S.J., Humphries, R.K., Lansdorp, P.M., Eaves, A.C. & Eaves, C.J. Quantitative assay for totipotent reconstituting hematopoietic stem cells by a competitive repopulation strategy. *Proc. Natl. Acad. Sci. USA* **87**, 8736–8740 (1990).
23. Lagasse, E. & Weissman, I.L. Flow cytometric identification of murine neutrophils and monocytes. *J. Immunol. Methods* **197**, 139–150 (1996).
24. Taniuchi, I. *et al.* Differential requirements for Runx proteins in CD4 repression and epigenetic silencing during T lymphocyte development. *Cell* **111**, 621–633 (2002).
25. Mikkola, H.K. *et al.* Haematopoietic stem cells retain long-term repopulating activity and multipotency in the absence of stem-cell leukaemia SCL/tal-1 gene. *Nature* **421**, 547–551 (2003).
26. Yagi, T. *et al.* A novel ES cell line, TT2, with high germline-differentiating potency. *Anal. Biochem.* **214**, 70–76 (1993).
27. Breton-Gorius, J., Reyes, F., Duhamel, G., Najman, A. & Gorin, N.C. Megakaryoblastic acute leukemia: identification by the ultrastructural demonstration of platelet peroxidase. *Blood* **51**, 45–60 (1978).
28. Jackson, C.W., Brown, L.K., Somerville, B.C., Lyles, S.A. & Look, A.T. Two-color flow cytometric measurement of DNA distributions of rat megakaryocytes in unfixed, unfractionated marrow cell suspensions. *Blood* **63**, 768–778 (1984).
29. Sherwood, S.W. & Schimke, R.T. Cell cycle analysis of apoptosis using flow cytometry. *Methods Cell Biol.* **46**, 77–97 (1995).

MOLECULAR AND CELLULAR BIOLOGY, Apr. 2004, p. 3227–3237 Vol. 24, No. 8
0270-7306/04/$08.00+0 DOI: 10.1128/MCB.24.8.3227–3237.2004


# Leukemia-Related Transcription Factor TEL Is Negatively Regulated through Extracellular Signal-Regulated Kinase-Induced Phosphorylation

Kazuhiro Maki,[1] Honoka Arai,[1] Kazuo Waga,[1] Ko Sasaki,[1] Fumihiko Nakamura,[1] Yoichi Imai,[2] Mineo Kurokawa,[2] Hisamaru Hirai,[2] and Kinuko Mitani[1]*

*Department of Hematology, Dokkyo University School of Medicine, Mibu-machi, Shimotsuga-gun, Tochigi 321-0293,[1] and Department of Hematology and Oncology, Graduate School of Medicine, University of Tokyo, Bunkyo-ku, Tokyo 113-8655,[2] Japan*

Received 25 April 2003/Returned for modification 17 July 2003/Accepted 13 January 2004

**TEL is an ETS family transcription factor that possesses multiple putative mitogen-activated protein kinase phosphorylation sites. We here describe the functional regulation of TEL via ERK pathways. Overexpressed TEL becomes phosphorylated in vivo by activated ERK. TEL is also directly phosphorylated in vitro by ERK. The inducible phosphorylation sites are $Ser^{213}$ and $Ser^{257}$. TEL binds to a common docking domain in ERK. In vivo ERK-dependent phosphorylation reduces *trans*-repressional and DNA-binding abilities of TEL for ETS-binding sites. A mutant carrying substituted glutamates on both $Ser^{213}$ and $Ser^{257}$ functionally mimics hyperphosphorylated TEL and also shows a dominant-negative effect on TEL-induced transcriptional suppression. Losing DNA-binding affinity through phosphorylation but heterodimerizing with unmodified TEL could be an underlying mechanism. Moreover, the glutamate mutant dominantly interferes with TEL-induced erythroid differentiation in MEL cells and growth suppression in NIH 3T3 cells. Finally, endogenous TEL is dephosphorylated in parallel with ERK inactivation in differentiating MEL cells and is phosphorylated through ERK activation in Ras-transformed NIH 3T3 cells. These data indicate that TEL is a constituent downstream of ERK in signal transduction systems and is physiologically regulated by ERK in molecular and biological features.**

TEL is a member of the ETS family transcription factors (7) that are essential for a variety of developmental processes and cellular responses to environmental stimuli. TEL shares with other ETS proteins an evolutionarily conserved ETS domain at the C terminus that is responsible for DNA binding to the ETS-binding consensus site (EBS) (26). TEL also contains an N-terminal domain that is referred to as the helix-loop-helix (HLH), or pointed, domain. The HLH domain in TEL has the unique property of inducing its stable homodimerization or heterodimerization with other ETS family members (9, 13, 18, 27). Being a transcriptional repressor, TEL is known to interact with the relevant cofactors mSin3A and N-CoR (34). By interacting with histone deacetylase-3 directly or indirectly, TEL is believed to mediate transcriptional repression of target genes such as *FLI-1* (21), *Id1* (R. Martinez and T. R. Golub, Abstr. 42nd Annu. Meet. Am. Soc. Hematol., abstr. 453a, 2000), and *stromelysin-1* (6).

Various 12p13 translocations involving the *TEL* gene and generating the *TEL*-related chimeric genes have been reported in many types of hematological malignancies. In some translocations, receptor-type or non-receptor-type tyrosine kinases are fused to the N-terminal portion of TEL and are thus activated by homodimerization through the HLH domain in the TEL moiety. Examples include platelet-derived growth factor receptor β in t(5;12)(q33;p13) (12), ABL in t(9;12)(q34;p13) (8), JAK2 in t(9;12)(p24;p13) (19), and Syk in t(9;12)(q22;p13) (16). In other translocations, transcription factors are structurally and functionally modified by fusion with the N- or C-terminal part of TEL. Examples include AML1 in t(12;21)(p13;q22) (5, 10, 11) and MN1 in t(12;22)(p13;q11) (3). Thus, perturbation of original functions of the partner genes could be a mechanism in causing leukemia in patients with such translocations. On the other hand, tumor-suppressive functions of TEL are suggested, because the expression of TEL in Ras-transformed NIH 3T3 cells inhibits cell growth in liquid and soft agar cultures (6, 32).

TEL is widely expressed throughout mouse embryonic development and in most human and mouse tissues. It is essential for mouse development, since its inactivation by homologous recombination results in embryonic lethality at E10.5 to E11.5 (35). The knockout embryos show defects in yolk sac angiogenesis and intraembryonic apoptosis of mesenchymal and neural cells, while they present normal yolk sac hematopoiesis. Analysis of chimeric mice with $TEL^{-/-}$ embryonic stem cells uncovered an essential role of TEL in establishing hematopoiesis of all lineages in neonatal bone marrow, although $TEL^{-/-}$ embryonic stem cells contributed to both primary and definitive fetal hematopoiesis (36). As for lineage-specific roles in hematopoietic systems, we have recently reported that TEL accelerates erythroid differentiation of mouse erythroleukemia (MEL) cells induced by hexamethylene bisacetamide (HMBA) or dimethyl sulfoxide (33).

* Corresponding author. Mailing address: Department of Hematology, Dokkyo University School of Medicine, 880 Kitakobayashi, Mibu-machi, Shimotsuga-gun, Tochigi 321-0293, Japan. Phone: 81-282-86-1111, ext. 2744. Fax: 81-282-86-5630. E-mail: kinukom-tky@umin.ac.jp.

Extracellular signal-regulated kinase (ERK) is one of the mitogen-activated protein kinases (MAPKs) that ubiquitously phosphorylate proline-directed serine/threonine residues and participate in signal transduction pathways controlling intracellular events (4, 14, 25). ERK governs mainly proliferation, differentiation, and cell survival through being activated by a wide range of cytokine and growth factor stimuli. Several nuclear transcription factors have been identified as in vivo substrates for MAPKs, molecular functions of which are altered through phosphorylation. TEL is also a nuclear phosphoprotein that possesses multiple putative MAPK phosphorylation sites (26). However, the functional significance of the phosphorylation has not yet been elucidated. In the present study, we investigated the regulation of TEL's functions through ERK-induced phosphorylation. TEL became phosphorylated by ERK on two serine residues, $Ser^{213}$ and $Ser^{257}$, in the internal domain between the HLH and ETS domains. TEL lost its abilities to repress transcription through the phosphorylation. A glutamate mutant molecularly mimicking hyperphosphorylated TEL also completely blocked TEL-mediated erythroid differentiation in MEL cells and antagonized TEL-induced growth suppression in H-Ras-transformed NIH 3T3 cells. Importantly, endogenous TEL proteins were found to be dephosphorylated in parallel with ERK inactivation during erythroid differentiation in MEL cells and to be phosphorylated by activated ERK in H-Ras-transformed NIH 3T3 cells. These results suggest that TEL's biological functions could be physiologically regulated through ERK-induced phosphorylation via various differentiation and proliferation signals.

## MATERIALS AND METHODS

**Plasmid construction.** pME18S-FLAG-TEL, pCXN2-FLAG-TEL, pME18S-FLAG-ΔHLH-TEL, pME18S-FLAG-Δ5'ID-TEL, pME18S-FLAG-ΔETS-TEL, pME18S-FLAG-ΔHLH+5'ID-TEL, pME18S-FLAG-ΔHLH+ID-TEL, and pME18S-EVI-1 were described previously (1, 33). The TEL mutants S22, S213, S238, and S257 were obtained by leaving the serine residues of the amino acids indicated and replacing the remaining residues among $Ser^{22}$, $Ser^{213}$, $Ser^{238}$, and $Ser^{257}$ with alanines in pME18S-FLAG-TEL by using the Chameleon double-stranded site-directed mutagenesis kit (Stratagene). The TEL mutants E22, E213, E238, E257, E213/238, E238/257, E213/257, E22/257, E22/213/257, and E213/238/257 were also obtained by replacing the serine residues of the amino acids indicated with glutamates in pME18S-FLAG-TEL. Both FLAG-tagged wild-type TEL and E213/257 mutant cDNAs were cloned into the EcoRI site of pCDNA3 (Invitrogen) and pSRαMSVtkneo retrovirus vector. FLAG-tagged wild-type TEL and S22, S213, S238, and S257 mutant cDNAs were cloned into the EcoRI site of pGEX-1 (Pharmacia). FLAG-tagged E213/257 mutant and influenza virus hemagglutinin (HA)-tagged wild-type TEL cDNAs were also cloned into the EcoRI site of the pCXN2 and the pCAGIpuro expression plasmids that carry the *neo*$^R$ and the *puromycin*$^R$ genes, respectively. pCMVMK, which is an expression vector of a rat ERK1-ERK2 chimeric protein, was described previously (31). To construct ERK-ΔCD, two Aor51HI sites (positions 915 and 996) were created by means of site-directed mutagenesis and the internal fragment from mutagenic Aor51HI (position 915) to mutagenic Aor41HI (position 996) was deleted. Activated H-Ras genomic DNA was purchased from JCRB GenBank and was cloned into the pCAGIPuro expression plasmid. The pGL2-754TR reporter plasmid contains a natural promoter derived from the *stromelysin-1* gene (6).

**Cell culture.** A Friend virus-induced erythroleukemia cell line, MEL-B8, and NIH 3T3 and COS-7 cells were maintained in Dulbecco's modified Eagle's medium (DMEM) supplemented with 10% fetal calf serum (FCS). To activate ERK, COS-7 cells were treated with 10% FCS plus 100 ng of recombinant human epidermal growth factor (EGF; Wakunaga) per ml after serum starvation with 0.1% FCS. To induce erythroid differentiation in MEL cells, 5 mM HMBA (Sigma-Aldrich) was added to the culture. Erythroid differentiation was determined by calculating the percentage of hemoglobin-producing cells following benzidine staining.

**Isolation of stable transfectants.** To establish stable transfectants of wild-type TEL or the E213/257 mutant, $1 \times 10^7$ MEL cells were electroporated with 20 μg of each cDNA cloned into the pCXN2 plasmid at 380 V and 975 μF by using Gene Pulser (Bio-Rad). Transfected cells were selected with 0.8 mg of G418 (Sigma-Aldrich)/ml and cloned by limiting dilution. Survival clones were screened for the expression of wild-type TEL or the E213/257 mutant by Western analysis with anti-FLAG M2 antibody (Sigma-Aldrich). To further obtain double transfectants of the wild-type-TEL and the E213/257 mutant, $2 \times 10^6$ MEL cells stably expressing the E213/257 mutant were electroporated with 8 μg of wild-type TEL cDNA cloned into the pCAGIpuro plasmid at 500 V and 25 μF by using Gene Pulser. Electroporated cells were selected with 0.75 μg of puromycin (Sigma-Aldrich)/ml and cloned by limiting dilution. Survival clones were screened for concomitant expression of the wild-type TEL and the E213/257 mutant by Western analysis with anti-HA (BAbCO) and anti-FLAG M2 antibodies. To establish stable transfectants expressing the activated H-Ras mutant, $5 \times 10^5$ NIH 3T3 cells were transfected with 10 μg of the pCAGIPuro-H-Ras expression plasmid by the Lipofectin method with TransFast (Promega). Transfected cells were selected with 0.3 μg of puromycin/ml and cloned by limiting dilution. Survival clones were screened for the expression of H-Ras by Western analysis with anti-H-Ras F235 antibody (Santa Cruz Biotechnology).

**Western analysis and immunoprecipitation.** COS-7 cells were transfected with FLAG-tagged wild-type TEL or its mutant expression plasmids alone or in combination with ERK expression plasmid by the DEAE-dextran method as described previously (33). Western analyses were performed as described previously (22) by using anti-FLAG M2, anti-HA, anti-ERK1 C-16 (Santa Cruz Biotechnology), or anti-phosphorylated ERK E10 (New England BioLabs) antibody. The blots were visualized by using the Problot AP system (Promega). Immunoprecipitation was carried out with anti-FLAG M2 or anti-TEL N-19 (Santa Cruz Biotechnology) antibody conjugated with protein G-Sepharose (Pharmacia), and immunoprecipitates were analyzed by sodium dodecyl sulfate-polyacrylamide gel electrophoresis (SDS-PAGE).

**Metabolic labeling.** COS-7 cells were cultured for 36 h after transfection in DMEM containing 10% FCS, transferred to DMEM containing 0.1% FCS, and incubated for 12 h. They were then transferred and cultured for 3 to 4 h in methionine- or phosphate-free DMEM supplemented with 0.1% FCS (dialyzed against 150 mM NaCl) plus 100 μCi of [$^{35}$S]methionine (Tran-$^{35}$S label; ICN)/ml or 400 μCi of [$^{32}$P]orthophosphate (Phosphorus-32; Amersham)/ml. Then, they were either left untreated or treated with 10% FCS (dialyzed against 150 mM NaCl) plus 100 ng of recombinant human EGF per ml for 5 min.

Parental MEL cells were cultured in DMEM containing 10% FCS with 5 mM HMBA for the indicated periods and were then transferred and cultured for 12 h in methionine- or phosphate-free DMEM supplemented with 10% FCS (dialyzed against 150 mM NaCl) plus 100 μCi of [$^{35}$S]methionine/ml or 400 μCi of [$^{32}$P]orthophosphate/ml.

After incubation in DMEM containing 10% FCS for 36 h, nontransformed or H-Ras-transformed NIH 3T3 clones were transferred and cultured for 12 h in methionine- or phosphate-free DMEM without FCS but with 100 μCi of [$^{35}$S]methionine/ml or 400 μCi of [$^{32}$P]orthophosphate/ml.

**In vitro kinase and pull-down assays.** Glutathione *S*-transferase (GST)-wild-type-TEL, S22, S213, S238, and S257 proteins were produced as described previously (17). For an in vitro kinase assay, COS-7 cells that were transfected with ERK expression plasmid were stimulated with EGF as described above. Cell lysates were immunoprecipitated with anti-ERK1 antibody conjugated with protein G-Sepharose and subjected to an in vitro kinase reaction with myelin basic proteins (MBPs) (Sigma-Aldrich) or GST-wild-type-TEL, S22, S213, S238, and S257 fusion proteins as a substrate as described previously (1). A pull-down assay was performed with GST-wild-type-TEL and COS-7 lysates expressing ERK or ERK-ΔCD as described previously (1).

**Luciferase assay.** NIH 3T3 cells were transfected with 1 μg of the pGL2-754TR reporter plasmid alone or along with 1 μg of expression plasmids by using TransFast (Promega). Luciferase assays were performed using the Dual-Luciferase reporter assay system (Promega) as described previously (1). We confirmed that all of the proteins used in this study were expressed at almost similar levels (data not shown).

**EMSA.** COS-7 cells were transfected with TEL expression plasmid alone or along with ERK expression plasmid and either left untreated or treated with EGF. Wild-type TEL and E213/257 mutant proteins were in vitro translated with pCDNA3 expression plasmids by using the TNT coupled wheat germ extract system (Promega). The procedures for the electrophoretic mobility shift assay (EMSA) and the oligonucleotides used were reported previously (33).

**Viral infection.** To prepare the retrovirus stocks, 10 μg of pSRαMSVtkneo, pSRαMSVtkneo-TEL, or pSRαMSVtkneo-E213/257 construct was transfected with 40 μg of ψ packaging plasmid into $1 \times 10^6$ COS-7 cells by the DEAE-

dextran method. The culture medium containing viruses was harvested 96 h after transfection. Viral titers were determined and normalized. Viral infections were carried out by exposing $5 \times 10^4$ H-Ras-transformed NIH 3T3 cells to 1 ml of virus stocks for 8 h. G418-resistant populations were selected in medium containing 0.4 mg of G418/ml after additional incubation for 48 h in medium without G418. The following experiments were performed with uncloned cell populations.

**Transformation assay.** For a soft agar assay, cells of each transfected derivative were trypsinized, suspended in DMEM containing 0.3% agar and 20% FCS, and plated onto a bottom layer containing 0.6% agar. Cells were plated at a density of $2 \times 10^4$ cells/3.5-cm dish in quadruplicate, and colonies >0.125 mm in diameter were enumerated after 14 days. The numbers of colonies are presented as mean values.

## RESULTS

**TEL is phosphorylated in vivo with dependence on activation of ERK.** MAPK-induced phosphorylation of several transcription factors is frequently detected as size-shifted bands of the proteins with SDS-PAGE (30). To clarify a role of TEL in the Ras/ERK signaling pathways, we examined whether TEL becomes phosphorylated through the activation of ERK. We observed three differently migrating bands (two slow-migrating bands and one fast-migrating band) derived from TEL in Western analysis, when TEL expression plasmid was introduced into COS-7 cells (Fig. 1A). Interestingly, overexpressed TEL showed a size shift when COS-7 cells cotransfected with ERK expression plasmid were serum starved and stimulated with EGF. Then, kinase activities of endogenous or overexpressed ERK in COS-7 cells were evaluated by an in vitro kinase assay with immunoprecipitates with anti-ERK antibody and its known substrate MBP (Fig. 1B). Endogenous ERK was slightly activated upon EGF stimulation, as judged by the phosphorylation status of MBP. The most prominent ERK activity was detected when ERK-transfected COS-7 cells were treated with EGF. We thus concluded that the EGF treatment potentiated kinase activities of overexpressed ERK in COS-7 cells. Therefore, TEL seems to be phosphorylated through the activation of ERK. To confirm in vivo phosphorylation of TEL proteins by activated ERK, we next employed [$^{35}$S]methionine and [$^{32}$P]orthophosphate labeling. FLAG-tagged TEL was transiently expressed with or without overexpressed ERK in COS-7 cells and immunoprecipitated with anti-FLAG antibody. With [$^{35}$S]methionine labeling, we observed two TEL-derived bands (a broad slow-migrating band and a narrow fast-migrating band) when only TEL was overexpressed (Fig. 1C). We also detected size-shifted bands when cotransfected ERK was stimulated with EGF. When [$^{32}$P]orthophosphate labeling was carried out, the former slow- and fast-migrating bands turned out to be derived from phosphorylated and unphosphorylated forms of TEL, respectively. The latter shifted bands appeared to be derived from hyperphosphorylated forms. These data indicate that approximately two-thirds of overexpressed TEL molecules are constitutively phosphorylated and that almost all of them are inducibly hyperphosphorylated upon ERK activation.

**ERK-dependent phosphorylation at Ser$^{257}$ is detectable as a size shift.** Overexpressed TEL proteins were detected as three differently migrating bands in COS-7 cells by Western analysis (Fig. 1A). In contrast to the results of the [$^{35}$S]methionine- and [$^{32}$P]orthophosphate-labeling experiments, two slow-migrating bands were considered to be derived from phosphorylated

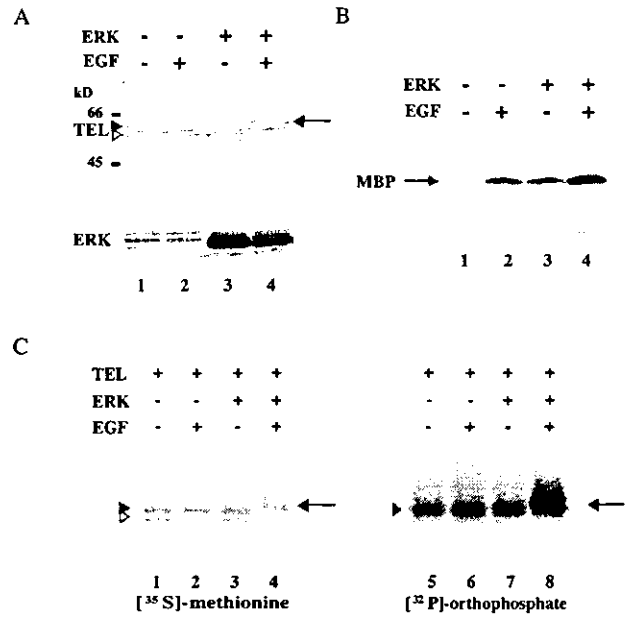


FIG. 1. (A) TEL shows a size shift upon activation of ERK. COS-7 cells were transfected with 5 μg of pME18S-FLAG-TEL alone (lanes 1 and 2) or together with 5 μg of pCMVMK (ERK expression plasmid) (lanes 3 and 4), starved in medium containing 0.1% FCS, and either left untreated (lanes 1 and 3) or treated with recombinant human EGF for 5 min (lanes 2 and 4). Western analyses were performed with anti-FLAG or anti-ERK1 antibody. (B) ERK activities in COS-7 cells. COS-7 cells were not transfected (lanes 1 and 2) or transfected with 5 μg of ERK expression plasmid (lanes 3 and 4) and treated as described for panel A. In vitro kinase assays were performed with MBP as a substrate. (C) [$^{35}$S]methionine and [$^{32}$P]orthophosphate labeling of TEL proteins. COS-7 cells were transfected with 5 μg of pME18S-FLAG-TEL alone (lanes 1, 2, 5, and 6) or together with 5 μg of ERK expression plasmid (lanes 3, 4, 7, and 8), subjected to metabolic labeling with [$^{35}$S]methionine (lanes 1 to 4) or [$^{32}$P]orthophosphate (lanes 5 to 8), treated as described for panel A, and immunoprecipitated with anti-FLAG antibody. Open arrowheads, solid arrowheads and solid arrows in panels A and C indicate unphosphorylated, phosphorylated, and hyperphosphorylated forms of TEL, respectively. Positions of size markers (in kilodaltons) are shown.

forms and a fast-migrating band was considered to be derived from unphosphorylated forms. The retarded bands that were observed when exogenous ERK was activated mirrored those of hyperphosphorylated forms. In order to determine phosphorylation sites in TEL, a set of deletion mutants (shown in Fig. 2A) were expressed with ERK in COS-7 cells and subsequently analyzed for size shifts after the EGF stimulation with SDS-PAGE. When three types of TEL mutants (ΔHLH-TEL, ΔHLH+5′ID-TEL, and ΔETS-TEL) were expressed in the presence of activated ERK, retarded bands were induced with almost the same pattern as in wild-type TEL (Fig. 2B). However, we did not detect such a size shift by ERK when ΔHLH+ID-TEL and Δ5′ID-TEL were expressed. These data suggest that major ERK-dependent phosphorylation sites exist within the region comprising amino acids 206 to 267 in TEL. We cannot completely rule out the existence of other phosphorylation sites outside this region because phosphorylation on some residues could not be detected as size shifts with SDS-PAGE.

Ser/Thr-Pro is a minimal consensus sequence for phosphor-

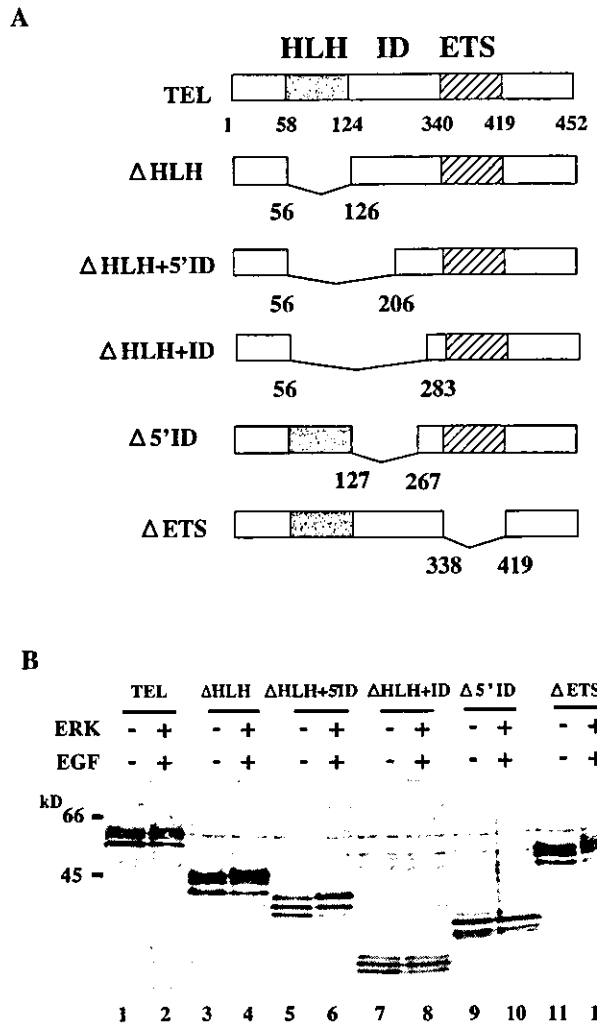


FIG. 2. (A) Structures of TEL deletion mutants. The HLH and the ETS domains are shown by shaded and hatched boxes, respectively. Numerals are amino acid numbers in the TEL protein. (B) ERK-dependent size shifts of wild-type TEL and its deletion mutants. COS-7 cells were transfected with 5 μg of pME18S-FLAG-TEL (lanes 1 and 2), pME18S-FLAG-ΔHLH-TEL (lanes 3 and 4), pME18S-FLAG-ΔHLH+5'ID-TEL (lanes 5 and 6), pME18S-FLAG-ΔHLH+ID-TEL (lanes 7 and 8), pME18S-FLAG-Δ5'ID-TEL (lanes 9 and 10), or pME18S-FLAG-ΔETS-TEL (lanes 11 and 12) alone (lanes 1, 3, 5, 7, 9, and 11) or in combination with 5 μg of ERK expression plasmid (lanes 2, 4, 6, 8, 10, and 12), serum starved, and either left untreated (lanes 1, 3, 5, 7, 9, and 11) or treated with recombinant human EGF for 5 min (lanes 2, 4, 6, 8, 10, and 12). Western analysis was performed with anti-FLAG antibody. Positions of size markers (in kilodaltons) are shown.

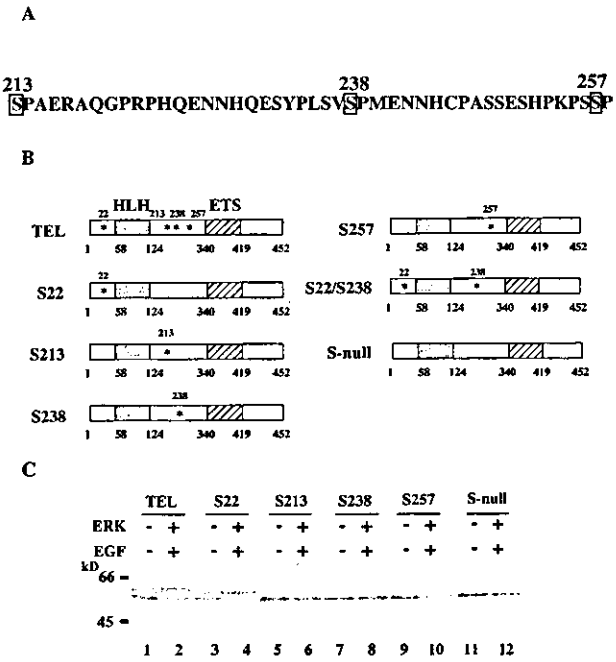


FIG. 3. (A) Potential sites of phosphorylation by ERK in TEL. Potential phosphorylation sites that meet a minimal consensus sequence (Ser/Thr-Pro) and reside within the region comprising amino acids 206 to 267 are boxed. Numerals are amino acid numbers in the TEL protein. (B) Structures of alanine mutants. The potential serine residues for phosphorylation, $Ser^{22}$, $Ser^{213}$, $Ser^{238}$, and $Ser^{257}$, were replaced with alanines. Asterisks show the positions of the residual serine residues. (C) ERK-dependent size shifts of wild-type TEL and its alanine mutants. COS-7 cells were transfected with 5 μg of pME18S-FLAG-TEL (lanes 1 and 2), pME18S-FLAG-S22 (lanes 3 and 4), pME18S-FLAG-S213 (lanes 5 and 6), pME18S-FLAG-S238 (lanes 7 and 8), pME18S-FLAG-S257 (lanes 9 and 10), or pME18S-FLAG-S-null (lanes 11 and 12) alone (lanes 1, 3, 5, 7, 9, and 11) or in combination with 5 μg of ERK expression plasmid (lanes 2, 4, 6, 8, 10, and 12) and treated as described in the legend to Fig. 2B. Western analysis was performed with anti-FLAG antibody. Positions of size markers (in kilodaltons) are shown.

ylation by all MAPKs (4). Thus, there are three potential phosphorylation sites ($Ser^{213}$, $Ser^{238}$, and $Ser^{257}$) within the region identified above if TEL is directly phosphorylated by ERK (Fig. 3A). Because $Ser^{22}$ is equivalent to $Thr^{38}$ in ETS1 and $Thr^{72}$ in ETS2 (29), which are phosphorylated by ERK (28, 38), this serine residue is another candidate for phosphorylation by ERK. To determine whether these four candidate sites become phosphorylated depending on ERK activation, we constructed TEL mutants S22, S213, S238, and S257 by leaving each serine residue as it is and replacing the remaining three residues with alanines by in vitro mutagenesis (Fig. 3B). In addition, we also constructed S-null, in which all four serine residues were replaced by alanines. Among these mutants, only S22 showed the slow- and fast-migrating bands that might correspond to phosphorylated and unphosphorylated forms of wild-type TEL without activated ERK, while the other four mutants, S213, S238, S257, and S-null, revealed only the fast-migrating bands and were thought to remain unphosphorylated (Fig. 3C). It is conceivable that almost two thirds of overexpressed wild-type TEL molecules are constitutively phosphorylated on $Ser^{22}$ without ERK activation. On the other hand, the S257 mutant showed the same pattern of shifted bands as wild-type TEL after ERK activation, while the remaining mutants hardly induced the shifted bands. Thus, $Ser^{257}$ may be a major phosphorylation site depending on ERK activation, and phosphorylation at $Ser^{213}$ and $Ser^{238}$ is not detectable by a size shift.

**TEL is directly phosphorylated by ERK in vitro at $Ser^{213}$ and $Ser^{257}$.** It is quite likely that TEL is directly phosphorylated by ERK, since the identified phosphorylation residue $Ser^{257}$ meets the minimal consensus sequence for phosphorylation by

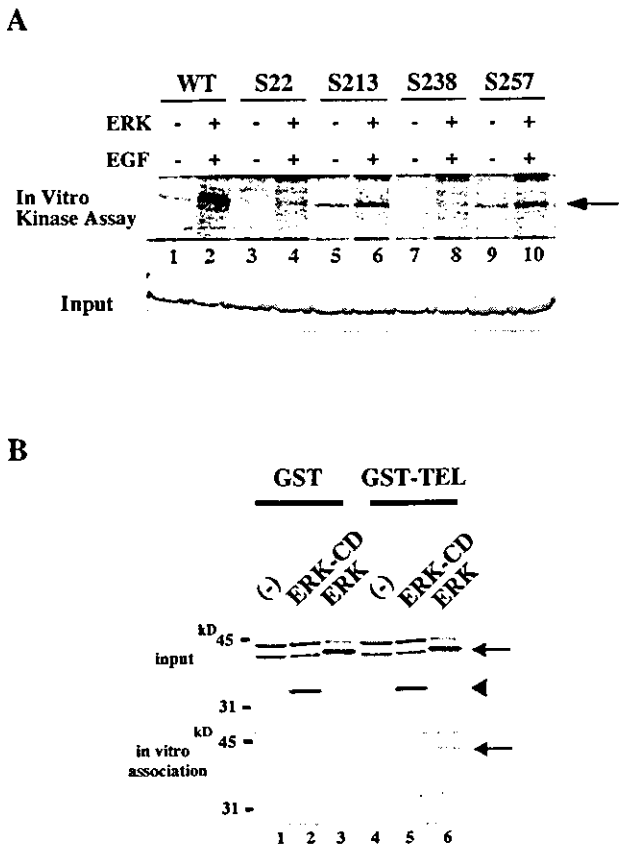


FIG. 4. (A) In vitro ERK kinase assays with wild-type TEL (WT), S22, S213, S238, and S257 as substrates. The top panel shows results of assays performed as described in the legend to Fig. 1. In the bottom panel, the input of each lane is shown by Coomassie staining. The arrow indicates GST-wild-type-TEL or its mutant fusion proteins phosphorylated by ERK. (B) Physical interaction between ERK and wild-type TEL through the CD domain in ERK. COS-7 cells were not transfected (lanes 1 and 4) or were transfected with 5 μg of ERK-ΔCD (lanes 2 and 5) or ERK (lanes 3 and 6) expression plasmid, harvested, and mixed with GST-glutathione-Sepharose beads (lanes 1 to 3) or GST-wild-type-TEL conjugated with glutathione-Sepharose beads (lanes 4 to 6). Western analyses were performed with anti-ERK antibody to detect ERK proteins expressed in COS-7 cells (top panel) and those bound to GST-wild-type-TEL (bottom panel). Arrows and a solid arrowhead indicate ERK and ERK-ΔCD proteins, respectively.

ERK. In order to confirm this possibility, a GST-wild-type-TEL fusion protein was produced in *Escherichia coli*, affinity purified, and used as a substrate for an in vitro ERK assay. ERK overexpressed in COS-7 cells was immunoprecipitated with anti-ERK antibody and subjected to the assay. GST-wild-type-TEL became phosphorylated in vitro by EGF-activated ERK (Fig. 4A). To determine phosphorylation sites in a more straightforward way, we next performed in vitro kinase assays with GST-S22, GST-S213, GST-S238, and GST-S257 fusion proteins. As expected from the Western analysis results described above, activated ERK induced phosphorylation in GST-S257 fusion protein in vitro. GST-S238 did not become phosphorylated at all, even after ERK activation, suggesting that neither $Ser^{238}$ nor any other serine or threonine residues except $Ser^{22}$, $Ser^{213}$, and $Ser^{257}$ are targets for ERK-induced phosphorylation. Surprisingly, GST-S213 became phosphorylated with activated ERK. This result indicates that $Ser^{213}$ is another phosphorylation site that is not detected as a band shift with SDS-PAGE. $Ser^{22}$, which was considered to be a constitutive phosphorylation site on the basis of SDS-PAGE analysis, became slightly phosphorylated upon ERK stimulation as with SDS-PAGE. Taking these results together, we conclude that both $Ser^{213}$ and $Ser^{257}$ in TEL are ERK-inducible phosphorylation sites.

**TEL physically interacts with ERK.** MAPKs have been reported to physically interact with some of their substrates through their common docking (CD) domains (30, 39). Thus, we investigated whether TEL associates with ERK depending on the CD domain. For this purpose, ERK and ERK-ΔCD, which lacks the entire CD domain, were overexpressed in COS-7 cells and their associations with immobilized GST-wild-type-TEL were examined. ERK significantly associated with GST-wild-type-TEL, but ERK-ΔCD did not (Fig. 4B). We conclude that ERK phosphorylates TEL by binding to it through the CD domain.

**ERK-dependent phosphorylation reduces *trans* repression by TEL.** In order to obtain insights into the functional modification of TEL through ERK-induced phosphorylation, we examined whether the phosphorylation alters the *trans*-repressional abilities of TEL through EBS. We employed the pGL2-754TR reporter (6), which contains a natural promoter derived from the TEL target gene *stromelysin-1*, in luciferase assays. A twofold decrease in luciferase activities was observed when wild-type TEL was expressed (Fig. 5A). However, both coexpression of ERK and treatment with EGF attenuated transcriptional suppression by wild-type TEL (Fig. 5A and B). A mutant with substituted alanines on both $Ser^{213}$ and $Ser^{257}$ (S22/238) was not influenced with regard to *trans*-repressional functions by either ERK overexpression or EGF treatment. From these data, we conclude that ERK-dependent phosphorylation inhibits transcriptional repression by TEL.

We constructed a set of TEL mutants by replacing some of the four candidate serine residues for phosphorylation with glutamates that mimic phosphoserine residues. Of these mutants, only the E213/257 and E22/213/257 mutants lost their abilities to repress the transcription through the pGL2-754TR reporter and functionally mimicked ERK-induced hyperphosphorylated TEL (Fig. 5C). Therefore, we speculate that phosphorylation at both $Ser^{213}$ and $Ser^{257}$ is required to modify TEL's molecular functions. Moreover, coexpression of the E213/257 mutant abolished the transcriptional suppression by wild-type TEL in a dose-dependent manner (Fig. 5D). When EVI-1 was coexpressed as a control, the repression by wild-type TEL was not affected at all. These data suggest that the E213/257 mutant exerts a dominant-negative effect on TEL-mediated transcriptional inhibition. We conclude that ERK-dependent phosphorylation negatively regulates TEL's abilities as a transcriptional repressor.

**ERK-dependent phosphorylation prevents DNA binding of TEL.** We thus examined whether hyperphosphorylated TEL still possesses EBS-specific DNA-binding properties like unmodified TEL does. Cell lysates prepared from COS-7 cells that were transfected with the empty pME18S plasmid (mock) or unstimulated wild-type TEL- or ERK-stimulated wild-type TEL-expressing COS-7 cells were subjected to EMSA with radioactive EBS oligonucleotide as a probe. Almost the same

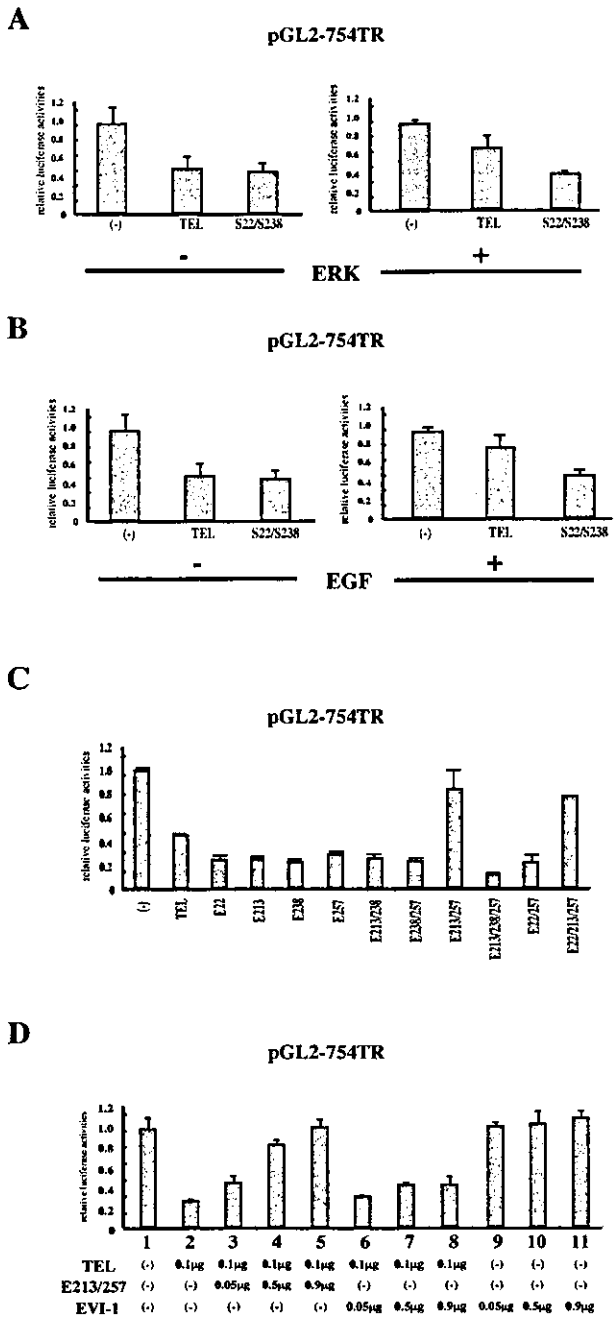


FIG. 5. (A) Overexpression of ERK inhibits TEL's *trans*-repressional ability. NIH 3T3 cells were transfected with 1 μg of the pGL2-754TR reporter plasmid alone or along with 0.5 μg of pME18S-FLAG-TEL or pME18S-FLAG-S22/S238 with or without 0.5 μg of ERK expression plasmid and cultured in DMEM containing 10% FCS for 48 h. (B) Activation of endogenous ERK also inhibits TEL's *trans*-repressional ability. NIH 3T3 cells were transfected with 1 μg of the pGL2-754TR reporter plasmid alone or along with 1 μg of pME18S-FLAG-TEL or pME18S-FLAG-S22/S238. After 48 h, the cells were incubated in DMEM containing 10% FCS with or without recombinant human EGF for 2 h before harvest. (C) Simultaneous replacement of $Ser^{213}$ and $Ser^{257}$ residues with glutamates eliminates TEL's *trans*-repressional ability. NIH 3T3 cells were transfected with 1 μg of the pGL2-754TR reporter plasmid alone or along with wild-type TEL or various kinds of TEL glutamate mutant expression plasmids and incubated for 48 h before harvest. (D) The glutamate mutant E213/257 shows a dominant-negative effect on TEL-mediated transcriptional repression. NIH 3T3 cells were transfected with 1 μg of the pGL2-754TR reporter plasmid alone (lane 1) or along with 0.1 μg of pME18S-FLAG-TEL (lanes 2 to 8). In lanes 3 to 8, 0.05, 0.5, and 0.9 μg of pME18S-FLAG-E213/257 or pME18S-EVI-1 were cotransfected as well. NIH 3T3 cells were also transfected with 1 μg of the pGL2-754TR reporter plasmid along with 0.05, 0.5, and 0.9 μg of pME18S-EVI-1 alone (lanes 9 to 11). Bars show luciferase activities relative to the level observed when control plasmid pME18S was cotransfected, and average results of duplicate experiments are presented.

amounts of TEL proteins were expressed in the lysates without and with ERK activation (Fig. 6A). As shown in Fig. 6A, unmodified TEL generated a specific DNA-protein complex that was supershifted with anti-TEL antibody and was hardly seen in the mock lysate. This band represented a specific binding of unmodified TEL to the EBS probe, since the binding was completely canceled by cold-specific competitors but not by nonspecific competitors. Notably, the specific DNA-protein band disappeared when TEL was hyperphosphorylated in vivo by activated ERK. These results indicate that ERK-dependent phosphorylation decreases the DNA binding of TEL.

We also compared the DNA-binding affinities of wild-type TEL and the E213/257 mutant by EMSA with in vitro-translated wild-type TEL and E213/257 mutant proteins. As shown in Fig. 6B, expression levels of wild-type TEL and E213/257 mutant proteins were almost similar. Wild-type TEL generated a specific DNA-protein complex that was completely canceled by cold-specific competitors but not by nonspecific competitors and was supershifted with two kinds of anti-TEL antibodies (N-19 and C-20). The band derived from the specific complex was quite broad, possibly because the association was extremely weak, and wild-type TEL proteins and the probe became dissociated during electrophoresis. However, the E213/257 mutant formed neither the specific DNA-protein complex nor the supershifted complex with either anti-TEL antibody. From these results, we conclude that the E213/257 mutant loses its ability for DNA binding to the EBS and conceivably mimics hyperphosphorylated TEL in DNA binding. The E213/257 mutant was found to bind to mSin3A and locate in the nucleus as wild-type TEL does (data not shown). Moreover, the glutamate mutant formed a homodimer and a heterodimer with wild-type TEL (data not shown). It could be possible that hyperphosphorylated TEL without DNA binding modulates molecular functions of nonhyperphosphorylated TEL by heterodimerizing with it.

**E213/257 mutant blocks erythroid differentiation in MEL cells and stimulates growth in H-Ras-transformed NIH 3T3 cells.** Considering that the E213/257 mutant has a dominant-negative effect on wild-type TEL-mediated transcriptional repression, we further analyzed alterations of TEL's biological functions through ERK-dependent phosphorylation. For this purpose, we employed MEL and NIH 3T3 cells. Because we have reported that overexpression of wild-type TEL accelerates erythroid differentiation induced by chemical compounds such as HMBA and dimethyl sulfoxide in MEL cells (33), we established clones expressing wild-type TEL, the E213/257 mutant, and both wild-type-TEL and the E213/257 mutant to test the effect of hyperphosphorylated TEL on erythroid differentiation. Figure 7A shows the expression of wild-type TEL